Journal of Rock Mechanics and Geotechnical Engineering 10 (2018) 486–512

Contents lists available at ScienceDirect

Journal of Rock Mechanics and Geotechnical Engineering

journal homepage: www.rockgeotech.org

Full Length Article

Analysis of unlined pressure shafts and tunnels of selected Norwegian hydropower projects

Chhatra Bahadur Basnet*, Krishna Kanta Panthi

Department of Geoscience and Petroleum, Norwegian University of Science and Technology, Sem Saelands Vei 1, NO-7491, Trondheim, Norway

ARTICLE INFO

Article history:
Received 19 September 2017
Received in revised form
7 December 2017
Accepted 25 December 2017
Available online 24 February 2018

Keywords:
Hydropower projects
Unlined pressure shafts and tunnels
Minor principal stress
Hydraulic jacking
Water leakage

ABSTRACT

Norwegian hydropower industry has more than 100 years of experiences in constructing more than 4000 km-long unlined pressure shafts and tunnels with maximum static head of 1047 m (equivalent to almost 10.5 MPa) reached at unlined pressure tunnel of Nye Tyin project. Experiences gained from construction and operation of these unlined pressure shafts and tunnels were the foundation to develop design criteria and principles applied in Norway and some other countries. In addition to the confinement criteria, Norwegian state-of-the-art design principle for unlined pressure shaft and tunnel is that the minor principal stress at the location of unlined pressure shaft or tunnel should be more than the water pressure in the shaft or tunnel. This condition of the minor principal stress is prerequisite for the hydraulic jacking/splitting not to occur through joints and fractures in rock mass. Another common problem in unlined pressure shafts and tunnels is water leakage through hydraulically splitted joints or pre-existing open joints. This article reviews some of the first attempts of the use of unlined pressure shaft and tunnel concepts in Norway, highlights major failure cases and two successful cases of significance, applies Norwegian criteria to the cases and reviews and evaluates triggering factors for failure. This article further evaluates detailed engineering geology of failure cases and also assesses common geological features that could have aggravated the failure. The minor principal stress is investigated and quantified along unlined shaft and tunnel alignment of six selected project cases by using three-dimensional numerical model. Furthermore, conditions of failure through pre-existing open joints by hydraulic jacking and leakage are assessed by using two-dimensional fluid flow analysis. Finally, both favorable and unfavorable ground conditions required for the applicability of Norwegian confinement criteria in locating the unlined pressure shafts and tunnels for geotectonic environment different from that of Norway are highlighted.

1. Introduction

Norway has built more than 200 underground powerhouses and 4200 km-long hydropower tunnels in the past 100 years (Broch, 2013). Experiences gained in design, construction and operation of waterway system have led to the development of innovative ideas. One of these ideas is the application of unlined high-pressure tunnels and shafts in hydropower schemes. It is estimated that over 95% of the waterway length of Norwegian hydropower schemes is left unlined (Johansen, 1984; Panthi, 2014). The earliest attempt to apply such concept in Norway was in Herlandsfoss project in 1919 (Vogt, 1922), and up to now, more than 4000 km-long unlined pressure shafts and tunnels with maximum static head of 1047 m have been in successful operation. Panthi and Basnet (2016) collected the information about most of the unlined tunnel projects and explained a brief history of development of unlined shaft and tunnel concept in Norway. They generalized the layout of such unlined shafts and tunnels in different hydropower schemes in four different arrangements, which are being practiced in Norway since the start of unlined pressure tunnel concept (Fig. 1). The arrangements shown in Fig. 1 are prepared based on the layout of a number of successful unlined shafts and tunnels in different hydropower schemes of Norway.

Apart from Norway, the unlined pressure tunnels are constructed worldwide where the layout planning, design and construction experiences from Norway are extensively used in

* Corresponding author.
E-mail address: chhatra.basnet@ntnu.no (C.B. Basnet).

Peer review under responsibility of Institute of Rock and Soil Mechanics, Chinese Academy of Sciences.

https://doi.org/10.1016/j.jrmge.2017.12.002

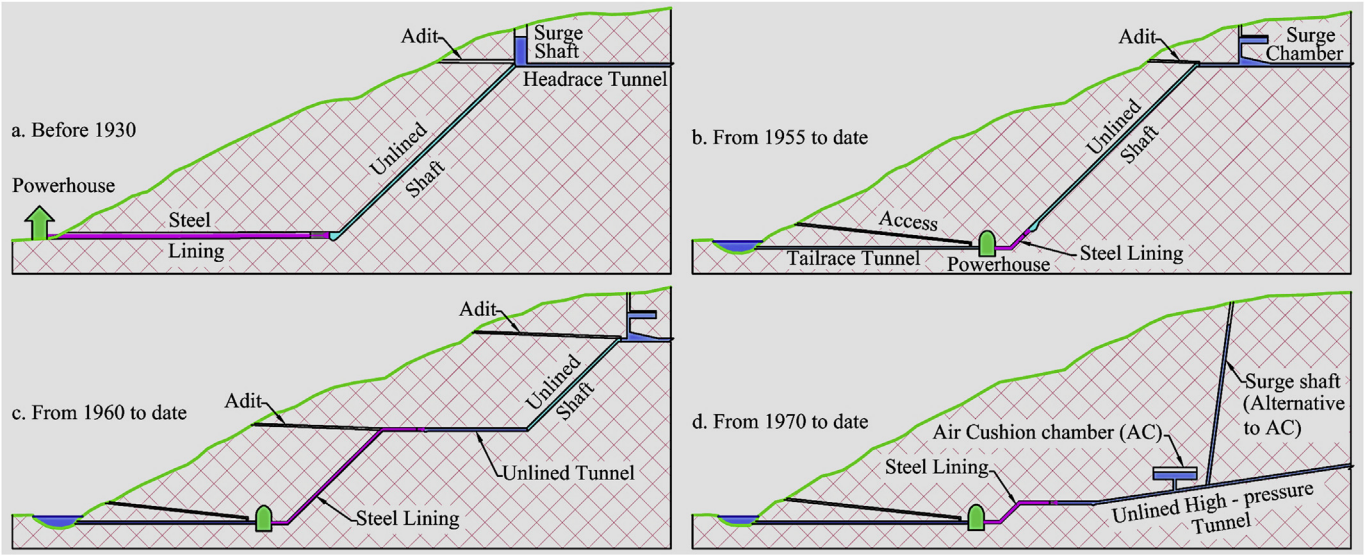

Fig. 1. Locations of unlined high-pressure shafts and tunnels in different hydropower schemes of Norway.

different geological and tectonic environments. Some examples of unlined pressure tunnels around the world are mentioned here. In Colombia, Chivor and Gauvio projects were planned with unlined pressure tunnels where Norwegian design principles were used in the design process (Broch, 1984; Broch et al., 1987). In Tanzania, unlined high-pressure tunnel of Lower Kihansi hydropower project was designed by using Norwegian criteria (Marwa, 2004). Palmstrom and Broch (2017) highlighted that two of the hydropower projects with unlined tunnels are in operation in Chile after the repair work of the collapses occurred after the waterway system is filled and power plants come in operation. Similarly, according to Norconsult (2017), the Las Lajas project in Chile is planned to use 9.5 km-long unlined pressure tunnel. In Portugal, Venda Nova II (Lamas et al., 2014) and Venda Nova III (Esteves et al., 2017) have successfully employed unlined pressure tunnels and both projects are in operation without any significant problem. In China, there is growing rate of use of unlined tunnels in the hydropower projects (Liu, 2013). In Nepal, Upper Tamakoshi Hydroelectric with unlined pressure tunnel is under construction (Panthi and Basnet, 2017) and is expected to be water-filled within two years of time.

The principle behind the idea of unlined pressure tunnel concept is that the rock mass itself works as a natural concrete against the pressure exerted by water column in the tunnel (Broch and Christensen, 1961; Selmer-Olsen, 1969; Broch, 1982). It is well known that Norway is geologically considered as a hard rock province, since two thirds of the country is situated in the Precambrian rocks consisting of gneisses (the most dominant rock type), granites, gabbros and quartzites. This hard rock province offers stiff rocks, which could work against the high water pressure without failure. However, about one third of the landscape is made up of rocks of Cambro-Silurian age (mainly Caledonian mountain range) consisting of different mixes of rock types such as gneisses, schists, phyllites, greenstones and marbles of varying degree of metamorphism as well as granites, gabbros, sandstones, shales, dolomites and limestones (Johansen, 1984). It is worthy to note here that waterway systems of many Norwegian hydropower schemes are aligned along the rock mass of the Caledonian mountain range, which do not represent as stiff rock mass as that of the Precambrian formations. The typical feature of Norwegian landscape is that the last deglaciation left the rock surface without any appreciable weathered material on the top of the surface, but there is a tendency of a frequent jointing in the rock mass near the surfaces. Selmer-Olsen (1969) explained that this condition may lead to higher permeability of rock mass at a depth ranging from 5 m to 40 m, which could cause water leakage. On the other hand, more stabilized tectonic setting (relatively few tectonic activities in comparison to other mountainous regions) helped to increase confinement in the rock mass even near surface. In general, favorable engineering geological and geotectonic environment of the Scandinavian landscape has favored the use of unlined pressure tunnel concept in Norway.

The successful history of the operation of unlined pressure shafts and tunnels in Norway is almost 99% with very few stability problems along the waterway system excluding some exceptions where problems were registered during the initial phase of the development of unlined concepts. The detailed studies of the failure were carried out and the lessons learned from the failure were helpful in developing certain design principles and criteria for unlined high-pressure tunnels and shafts (Broch and Christensen, 1961; Selmer-Olsen, 1969, 1974, 1985; Broch, 1982). In addition to the design criteria for confinement, a concept came in practice after the 1970s that nowhere along the unlined shafts and tunnels, the minor principal stress should be less than the pressure due to static water head. In order to use this concept in practice, a set of standard two-dimensional (2D) finite element charts were prepared in 1971–1972 for valley side slope from 14° to 75° (Nilsen and Thidemann, 1993). Bergh-Christensen (1982), Bergh-Christensen and Kjolberg (1982), Buen and Palmstrom (1982) and Benson (1989) emphasized the necessity of more detailed study on the engineering geological and stress state conditions. The in situ stress measurement program became popular means to verify the assumptions made during the design of unlined concept in Norway as well as in other parts of the world (Bergh-Christensen, 1982, 1986; Myrset and Lien, 1982; Vik and Tunbridge, 1986; Palmstrom, 1987; Hartmaier et al., 1998; Panthi and Basnet, 2017). The risk of hydraulic jacking along the pre-existing joints and fractures and possibility of leakage were always the major issues in the design of unlined tunnels and shafts (Barton et al., 1987; Brekke and Ripley, 1987). Hydraulic jacking test and fluid flow analysis through the joints could also be used to

assess the risk of hydraulic jacking and leakage (Ming and Brown, 1988; Edvardsson and Broch, 2002).

The above description clearly indicates that the detailed geological assessment, stress state analysis, hydraulic jacking, leakage analysis and in situ rock stress measurement should be carried out in addition to the use of design criteria for confinement and standard finite element charts. In this article, detailed geological assessment of seven major failure cases, stress state analysis of four failures and two successful cases and hydraulic jacking and leakage assessment of four failure cases have been carried out. The reliable application of standard 2D finite element charts is limited due to the uniqueness of each project in terms of topography and geology. In recent years, more sophisticated 2D computer programs are being used to model the project-specific topography and geology. However, 2D model in general fails to quantify the effect of complex topography and complex geology including intersecting faults and zones of weakness in the in situ stress state. In order to cope with this limitation, three-dimensional (3D) computer programs (FLAC^{3D}) is used in this article for the quantification of in situ stress state. In addition, 2D fluid flow model (UDEC) is used to assess the hydraulic jacking and water leakage through the pre-existing joints.

2. Brief description of the cases

As mentioned above, most of the unlined pressure tunnels and shafts in Norway are successfully operated without serious instability problems excluding few exceptions, which became the basis for the development of design principles and criteria. The Herlandsfoss was the first hydropower scheme built in 1919 to use unlined pressure shaft concept and followed by Skar and Svelgen built in 1920 and 1921, respectively (Vogt, 1922). Mixed experience was gained from these three projects with Skar completely failed and other two were brought in operation after needed mitigation measures. Most of the unlined pressure tunnels and shafts were successfully designed and operated until the failure that occurred at Byrte project in 1968 and at Askara project in 1970. The failure that took place at these two projects was instrumental in enhancing the design principles. Even though all unlined pressure shafts and tunnels follow the established design principles and criteria, there are still cases of failures even in modern time where further investigations were needed with substantial mitigation measures applied after the first water filling. The examples of such projects are Bjerka, Fossmark and Holsbru. However, the maximum static water head of 1047 m was successfully applied at unlined pressure tunnel of Nye Tyin project in 2004, which is the world record to date. Ten selected cases of the unlined pressure shaft and tunnel projects (eight failed and two highest head projects successfully implemented and operated) are listed in Table 1 for the purpose of detailed investigations and analysis in this paper.

The locations of the selected projects are shown in the overall geological map of Norway in Fig. 2. The projects such as Svelgen and Askara are located in Devonian sandstone whereas Byrte and Bjerka projects are situated in Archean and Proterozoic basements. The rest of the selected projects are situated in Caledonian rock formations. Each of the rock formations has different rock types, geological conditions and tectonic environments. The strength properties of different rocks are tested in the laboratory mostly by SINTEF and the database was published in SINTEF (1998).

The detailed geological conditions differ from project to project even though the projects are situated in same geological formations. Hence, the geological conditions are project-specific and have to be studied in detail for each project. The detailed information was collected for each selected project from the available project reports and the published articles. For in situ stress state analysis, the magnitude and orientation of horizontal stresses are needed. Fejerskov and Lindholm (2000) studied the mechanism of stress generation of the Norwegian continental shelf and compiled the stress database. Similarly, Hanssen (1997) also compiled the stress data including stress measurement in some of the hydropower projects. The required stress data were collected from Nilsen and Thidemann (1993), Fejerskov (1996), Hanssen (1997) and Myrvang (2017). The magnitude and orientation of horizontal stresses in and nearby the locations of selected projects are then superimposed in the geological map of Norway, as shown in Fig. 2.

3. Norwegian confinement criteria

According to Broch (1982), unlined pressure shafts and tunnels built in the 1950s and 1960s were designed using following rule of thumb:

$$h > cH \tag{1}$$

Table 1
Selected cases of unlined pressure shafts and tunnels in Norway.

Project	Location	Year	Gross head (m)	Maximum discharge (m^3/s)	Installed capacity (MW)	Maximum head in unlined shaft/tunnel (m)	Rock type	Failure condition and applied solution
Herlandsfoss	Osteroy, Hordaland	1919	136	6	12	136 (T)	Mica schist	Partly failed and steel lined
Skar	Tingvoll, More og Romsdal	1920	149	1	3.3	129 (T)	Granitic gneiss	Completely failed and steel lined
Svelgen	Bremanger, Sogn og Fjordane	1921	225	6.5	12	152 (S)	Sandstone	Minor leakage and concrete lined
Byrte	Tokke, Telemark	1968	295	8	20	295 (S)	Granitic gneiss	Partly failed and steel lined
Askara	Bremanger, Sogn og Fjordane	1970	690	11.4	85	200 (T)	Sandstone	Partly failed and steel lined
Bjerka	Hemnes, Nordland	1971	370	6.3	20	72 (T)	Gneiss	Partly failed and steel lined
Fossmark	Vaksdal, Hordaland	1985	440	2.38	9	380 (T)	Granite	Partly failed and steel lined
Naddevik	Ardal, Sogn og Fjordane	1987	963	–	112	963 (S)	Dark gneiss	Successfully operated
Nye Tyin	Ardal, Sogn og Fjordane	2004	1050	–	360	1047 (T)	Dark gneiss, granitic gneiss, phyllite and metasandstone	Successfully operated
Holsbru	Ardal, Sogn og Fjordane	2012	692	8.6	49	63 (T)	Dark gneiss	Leakage

Note: T = Tunnel; S = Shaft.
Sources: Vogt, 1922; Selmer-Olsen, 1969; Bergh-Christensen, 1975; Valstad, 1981; Broch, 1982; Buen, 1984; Vik and Tunbridge, 1986; Garshol, 1988; Panthi and Basnet, 2016.

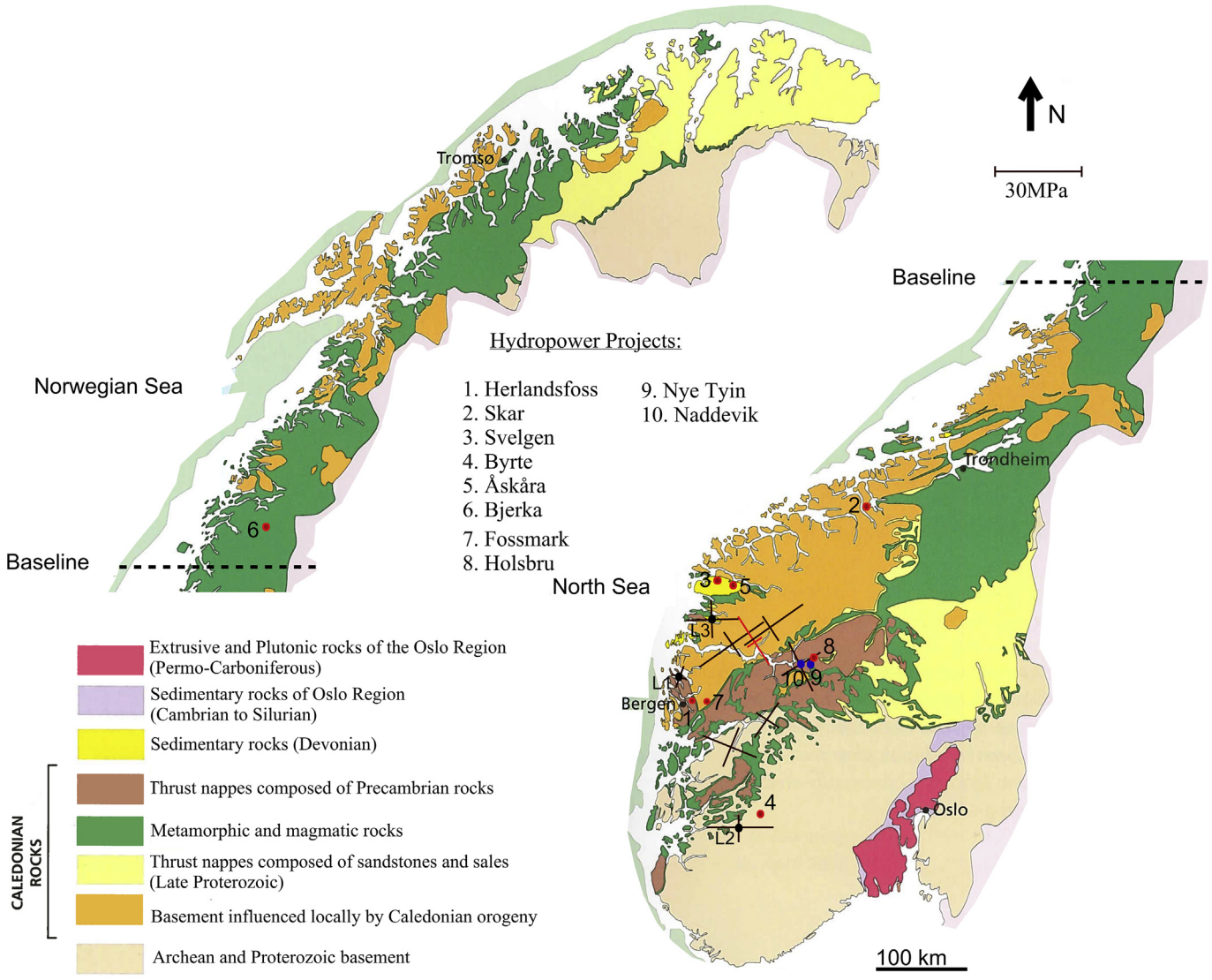

Fig. 2. Locations of the hydropower projects in the geological map of Norway with direction and magnitude of horizontal rock stresses superimposed (Map source: NGU, 2017).

where h is the minimum required rock cover over the shaft alignment, H is the hydrostatic head acting over the shaft alignment, and c is a constant that has a value of 0.6 for valley sides with inclinations up to 35° and 1 for valley sides slope exceeding 35°.

After the failure of unlined pressure shaft at Byrte in 1968 where the pressure shaft had an inclination of 60°, the rule of thumb expressed by Eq. (1) was upgraded as (Broch, 1982):

$$h > \frac{H}{\rho \cos \alpha} \tag{2}$$

$$\rho = \frac{\rho_r}{\rho_w} \tag{3}$$

where ρ_w is the density of water, ρ_r is the density of the rock, ρ is the relative density of the rock, and α is the inclination of shaft/tunnel with respect to horizontal plane. It is highlighted that if the shaft has an inclination more than 60°, Eq. (2) is no longer valid. In such situations, the shaft should be placed inside the line representing minimum depth for a 45° shaft (Selmer-Olsen, 1969).

The above design criterion was used in the design of unlined shafts in Norway until the failure at Askara in 1970. This failure led to the establishment of a new concept proposed by Bergh-Christensen and Dannevig (1971) that considers the shortest perpendicular distance (L) from the valley inclination line (Fig. 3), which is expressed by

$$L > \frac{H}{\rho \cos \beta} \tag{4}$$

where β represents the angle of valley side slope with respect to horizontal plane. Since then, both Eqs. (2) and (4) are considered as the state-of-the-art Norwegian rule of thumb for the confinement criterion of unlined/shotcrete-lined pressure shafts and tunnels.

It would be of great interest to check whether the cases mentioned above (Table 1) fulfill the design criteria expressed by Eqs. (2) and (4). The profiles along shaft and tunnel alignment for all these cases excluding Holsbru project are shown in Fig. 4 for the geometrical reference of locations to be investigated. However, all profiles shown in Fig. 4 represent critical sections defined by the needed rock cover and slope inclinations except for Askara,

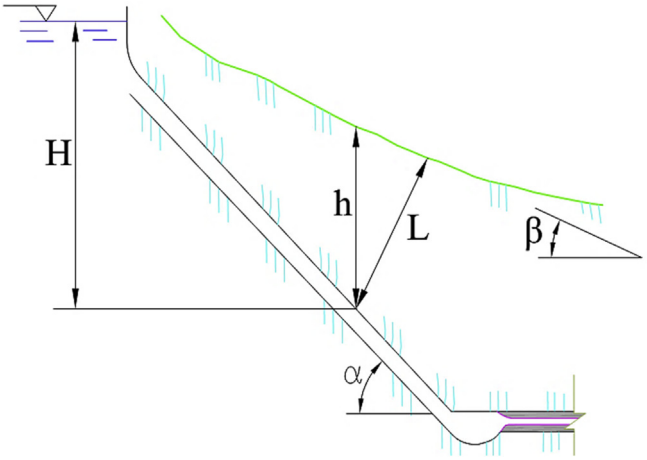

Fig. 3. Definition for the rule of thumb (Broch, 1982).

Naddevik and Nye Tyin projects. In these projects, respective critical sections are taken from 3D topography and the required geometrical information is extracted. While defining the valley side slope angle and measuring the available vertical rock cover (h') and available shortest distance (L'), a correction of valley side slope for protruding noses as recommended by Broch (1984) is applied. The details of the calculation including available factor of safety are presented in Table 2.

As seen in Table 2, the required vertical rock cover and shortest distance from the valley side slope at different locations of selected projects are calculated. The calculated values are compared with the actually available values to calculate the factor of safety (FoS_1 and FoS_2). In theory, the factor of safety should be greater than one for no failure to occur at the selected location of the unlined shaft and tunnel. It is interesting to note that there are locations (Sv-A, Bj-A, Br-A, Br-B, Br-C, As-A, Fo-B, Fo-C, Fo-D, Fo-E, Fo-F and Holsbru) where even though the factor of safety is greater than one, the failure/leakage was experienced after the water filling was carried out. On the other hand, in some locations (Hf-C, Sv-B and Br-D), no

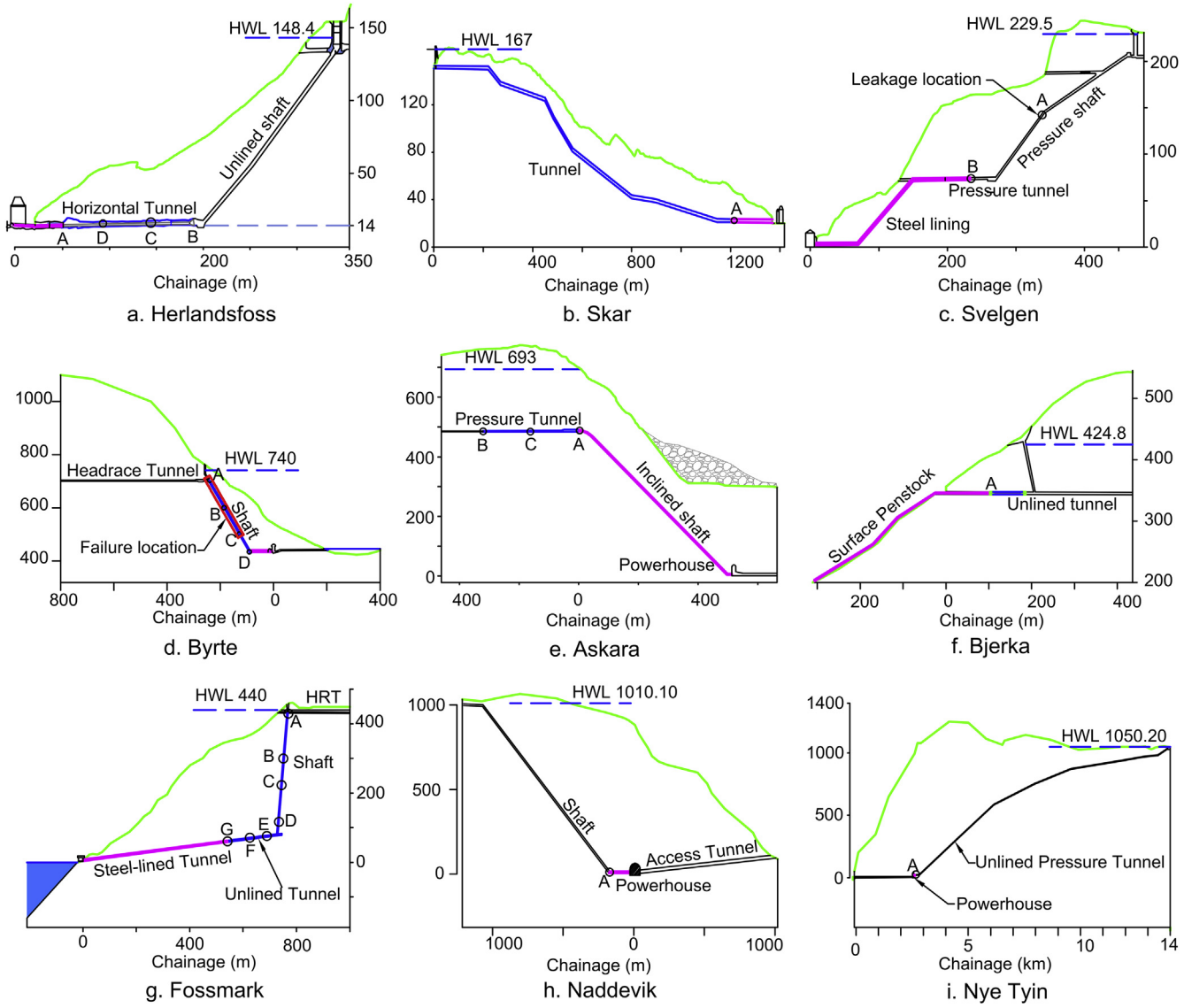

Fig. 4. Overview of profiles along the unlined shaft/tunnel of different hydropower projects in Norway. The vertical axis represents the elevation in masl (meter above sea level). HWL is the head water level.

Table 2
Analysis of the cases based on the design criteria defined by Eqs. (2) and (4).

Project	Location	H (m)	ρ_r (t/m^3)	h' (m)	α (°)	β (°)	L' (m)	L'/H	h (m)	L (m)	FoS_1 (h'/h)	FoS_2 (L'/L)	Remarks
Herlandsfoss	Hf-B	136	3.05	56	0	26	51	0.38	45	50	1.26	1.03	No failure
	Hf-C	136	3.05	31	0	26	32	0.24	45	50	0.7	0.65	No failure
	Hf-D	136	2.77	19	0	28	17	0.13	49	56	0.39	0.31	Failure
Skar	Sk-A	129	2.65	30	8	10	25	0.19	49	49	0.61	0.51	Failure
Svelgen	Sv-A	84	2.65	38	27	25	40	0.48	36	35	1.07	1.14	Minor leakage
	Sv-B	152	2.65	54	0	25	48	0.32	57	63	0.94	0.76	No failure
Byrte	Br-A	37	2.64	45	60	40	40	1.08	28	18	1.61	2.19	Failure
	Br-B	116	2.64	100	60	40	70	0.6	88	57	1.14	1.22	Failure
	Br-C	210	2.64	147	60	40	114	0.54	159	104	0.92	1.1	Failure
	Br-D	295	2.64	200	60	40	125	0.42	223	146	0.89	0.86	No failure
Askara	As-B	200	2.71	273	0	26	241	1.21	74	82	3.7	2.94	No failure
	As-C	200	2.71	265	0	35	216	1.08	74	90	3.59	2.4	No failure
	As-A	200	2.71	200	0	55	130	0.65	74	129	2.71	1.01	Failure
Bjerka	Bj-A	72	2.64	61	0	25	58	0.81	27	30	2.24	1.93	Failure
Fossmark	Fo-A	9	2.64	12	84	31	8	0.89	5	4	2.49	2.01	No failure
	Fo-B	135	2.64	132	84	31	114	0.84	72	60	1.83	1.91	Failure
	Fo-C	213	2.64	205	84	31	177	0.83	114	94	1.8	1.88	Failure
	Fo-D	318	2.64	304	84	31	262	0.82	170	141	1.78	1.86	Failure
	Fo-E	364	2.64	334	6	31	288	0.79	139	161	2.41	1.79	Failure
	Fo-F	373	2.64	292	6	31	252	0.68	142	165	2.06	1.53	Failure
	Fo-G	380	2.64	250	6	31	215	0.57	145	168	1.73	1.28	No failure
Naddevik	Nd-C	963	2.74	905	48	35	740	0.77	525	429	1.72	1.72	No failure
Nye Tyin	Nt-F	1047	2.84	838	1	18	875	0.84	369	388	2.27	2.26	No failure
Holsbru	Tunnel end	63	2.65	76	0	30	65	1.03	24	27	3.2	2.37	Leakage

failure occurred even though the factor of safety is less than one. The remaining locations (Hf-B, Hf-D, Sk-A, Br-C, As-B, As-C, Fo-A, Fo-G, Nd-A and Nt-A) that fulfill the design criteria had no failure evidence. Based on Eq. (4), NGI (1972) has recommended two demarcation curves (Fig. 5) expressed by the ratio of shortest length (L') to static head (H) with the valley slope angle (β) that should principally fulfill the criterion for no leakage to occur along those locations of the pressure tunnels falling above these two curves. The analyzed datasets of Table 2 are plotted in Fig. 5 to test the criterion. As seen in Fig. 5, the results achieved are mixed, indicating some locations lying above these two curves where have experienced substantial leakage and some locations lying below these two curves with no leakage.

This indicates that the design criterion expressed by Eq. (4) does not necessarily fulfill the demand for leakage conditions through the unlined pressure tunnels and shafts and needs to be carefully assessed for each individual case, since each alignment of the waterway is unique in itself. It is important that a comprehensive engineering geological assessment should be carried out while designing the unlined pressure tunnels.

4. Engineering geology of the cases

The Norwegian confinement criteria for the design of unlined tunnels and shafts are developed mainly based on 2D geometry of the topography. The rule of thumb does not take into account the

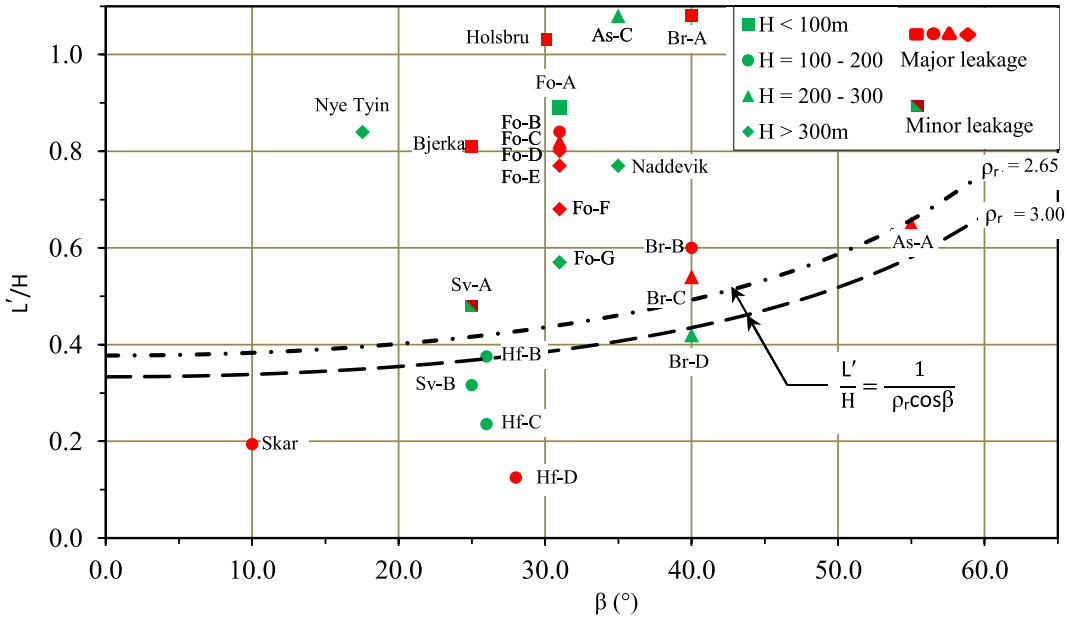

Fig. 5. Unlined pressure shafts and tunnels in valley side with various inclinations, β.

engineering geology and full overview of the in situ stress state of the area. The engineering geology includes rock types, strength properties of the rock and rock mass, joints and their characteristics, faults and zones of weakness presented along the shaft and tunnel alignment. In general, the stress state of the area is influenced by the 3D topography, weakness and fault zones, and the geotectonics and geological environment of the area. In the following, detailed engineering geology of the selected projects is assessed which is further used to quantify the input parameters required for the stress state analysis and hydraulic jacking assessment of the cases.

4.1. Herlandsfoss project

Herlandsfoss project has 1400 m-long headrace tunnel, surge shaft, inclined unlined shaft dipping approximately at 40°, and 175 m-long horizontal penstock tunnel near the powerhouse located at surface (Fig. 6). As indicated in Figs. 6 and 7, the main rock types in the project were registered as hornblende schist and mica schist and lay in the Caledonian nappe complex (Fig. 2). Hornblende schist was found to be massive and of good quality compared with the mica schist. A band of talcose mica schist passing through the southwest side of downstream valley was highly fractured.

The failure of unlined pressure tunnel of this project is explained in detail by Panthi and Basnet (2016) and the failure location at initially planned unlined tunnel is shown in Figs. 6 and 7. The failure resulted in excessive water leakage out from the tunnel, which was inferred as the occurrence of hydraulic jacking along the foliation joints of the highly schistose mica schist. The location of leakage area in the surface topography is also shown in Fig. 6. This hydraulic jacking that took place at the pressure tunnel led to extended existing joints in the rock mass and also new fractures were developed along the spring line of the unlined pressure tunnel over a distance of about 50 m from the initial cone area 'A'. It is worthwhile here to study this failure location in detail, since the failure had been noticed only in relatively weak mica schist even though the Norwegian criteria for confinement are not fulfilled in the nearby location with relatively stronger hornblende schist (Table 2).

The rock mass and jointing information is assessed and collected in the literature (e.g. Vogt, 1922; Broch and Christensen, 1961; NGI, 1972). Mica schist between chainage 55 m and 98 m was observed to be highly schistose and rich in chlorite and muscovite. The rock mass was found to be extremely schistose and was formed along the foliation joints, which has orientation of about N55°–60°W/46°–48°SW. The extent of schistosity was so high that even man's fingers could separate the fresh rock mass. In addition, the tunnel alignment met six marked calcite filled shear zones with strike ranging from N20°E to N40°E and dip ranging from 60°SE to 85°SE (Figs. 6 and 7). The shear zones presented had a width of 2–3 m and the joint spacing ranged between 5 cm and 20 cm, which were filled with calcite clay of 1–3 mm in thickness. Selmer-Olsen (1969) indicated that hornblende schist has some joints cross-cutting across the foliation planes. Broch and Christensen (1961) pointed out that the hydraulic jacking occurred along the joint sets 2–4 and along some foliation joints (Figs. 6 and 7) presented in schistose mica schist between chainage 55 m and 98 m.

4.2. Byrte project

Byrte project has low-pressure headrace tunnel, surge shaft, unlined pressure shaft (60° inclination), about 80 m-long steel lined horizontal tunnel, underground powerhouse and about 200 m-long tailrace tunnel, as shown in Fig. 8. Main rock type in the project is granitic gneiss. The rock mass consists of several systems of joint sets and minor faults/zones of weakness with strike approximately parallel to the valley side slope (Selmer-Olsen, 1969). There is also a wide clay-filled fault at Byrte Lake, which is called 'Byrte fault' (Figs. 8 and 9).

Fig. 9 shows the profile along the tunnel and shaft alignment with geological information included. According to Selmer-Olsen (1969), many cracks were observed in the rock mass both in the shaft and powerhouse cavern during the operation of power plant

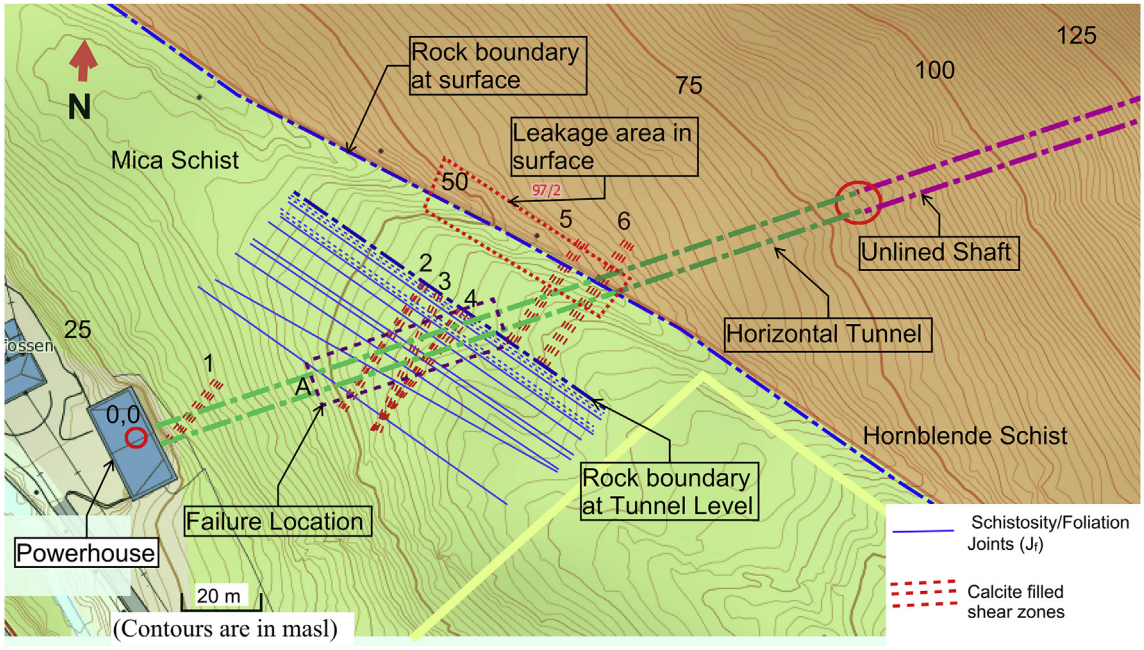

Fig. 6. The Herlandsfoss project details at failure location and rock formation (Contour map source: www.norgeskart.no).

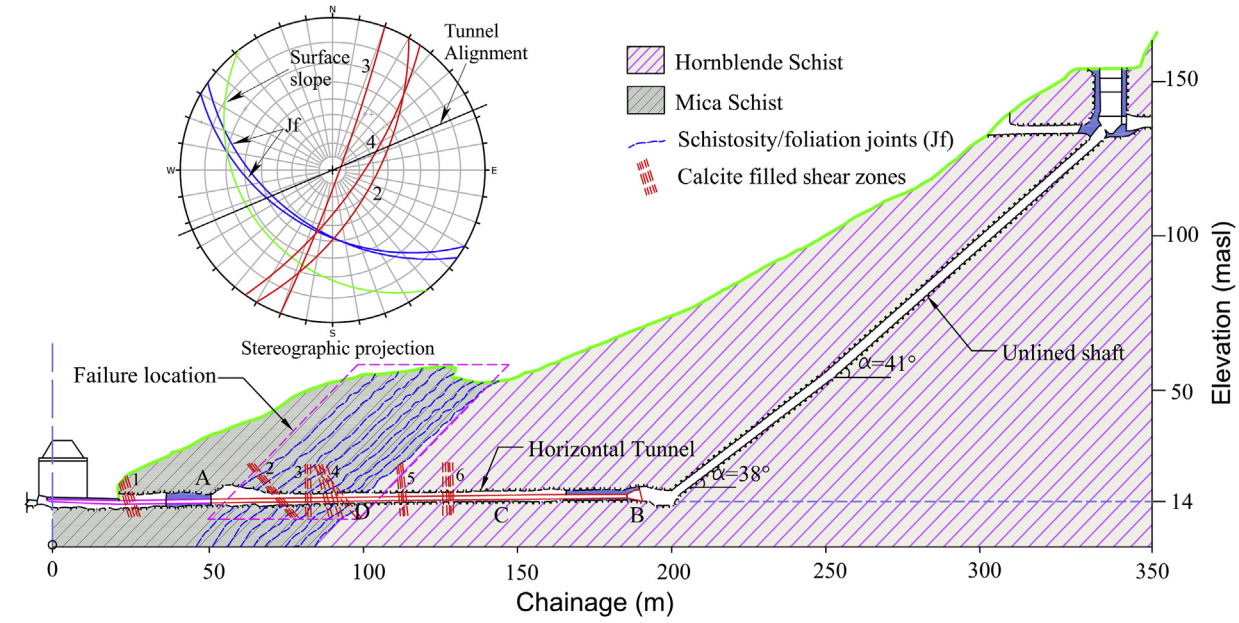

Fig. 7. Profile along the tunnel alignment and failure location of Herlandsfoss project.

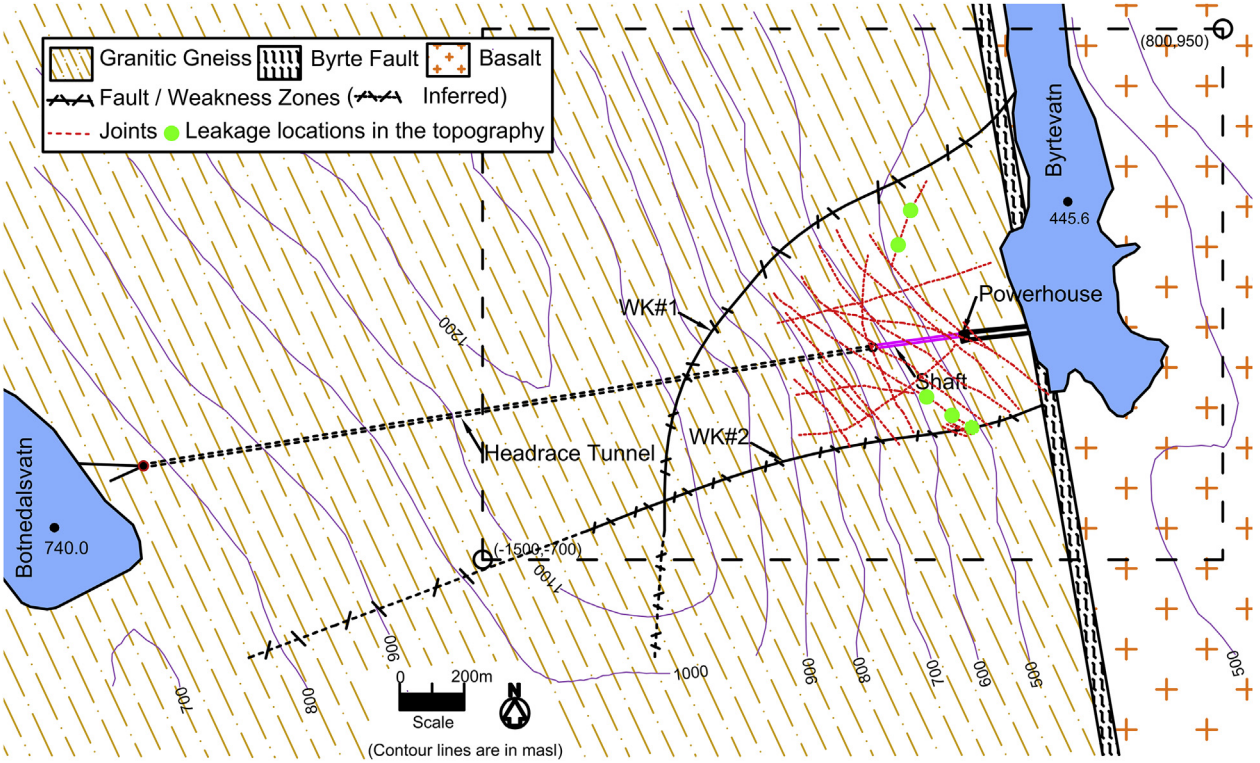

Fig. 8. Byrte project area with rock types, faults/zones of weakness, joints, and leakage locations.

at 300 m gross head. The cracks were marked above the zone of weakness (WK#1) in the shaft and to the right side of the zone of weakness along pressure tunnel to the powerhouse (NVE, 1970). There were no cracks along the shaft below the zone of weakness and the rock mass in this area was also observed as relatively massive and strong. Hence, it can be concluded that rock mass above the zone of weakness has more fractures and joints. Furthermore, leakage was experienced in underground powerhouse cavern and several springs also appeared at the surface topography indicating considerable leakage through the rock mass. The leakage locations in the surface topography are located in Fig. 8.

There are two joint systems in the project area. One of the joint sets, Joint#b in Fig. 9, has an average orientation of about N25°W/65°NE, which is almost parallel to the foliation joints. There are some representative joints shown in Fig. 9 (red color) along the

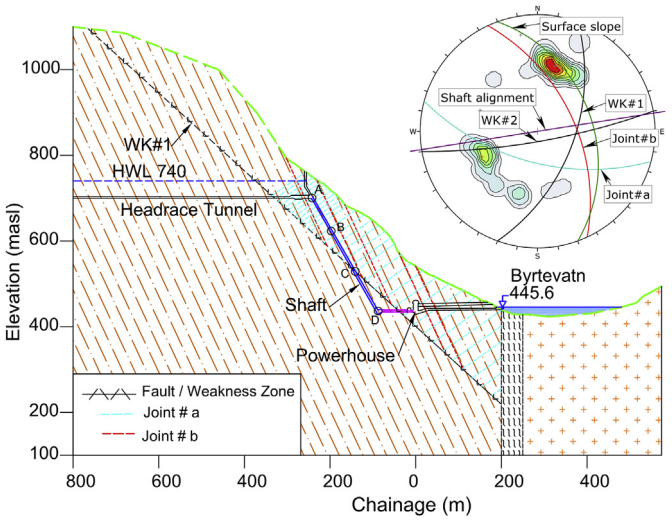

Fig. 9. Profile along the alignment of Byrte project and stereographic projection of joints, zones of weakness and shaft alignment.

shaft and tunnel alignment where hydraulic jacking occurred, since these joints have an opening of about 1–3 mm with almost no clay filling. Another joint set, Joint#a in Fig. 9, has an average orientation of about N75°W/60°SW with a spacing ranging between 10 m and 30 m and has joint opening of 0.5–3 mm. The joints observed in the area mostly open and the filled material if existed was washed away. In addition to these two joint sets, clay filled zones of weakness (WK#1 and WK#2) are also presented in Fig. 8. According to Selmer-Olsen (1969), the clay filled zone WK#1 in Fig. 9 constituting weak rock mass did not manage to sustain the hydrostatic head acting on it and hydraulic jacking occurred along this zone as well.

4.3. Askara project

The location and longitudinal profile of unlined tunnel and other project components of Askara project are shown in Figs. 10 and 11. Main rock type in the project is Devonian sandstone with bedding plane (Jb) striking about N30°E and dipping approximately 20°–25°SE (Bergh-Christensen, 1975). The rock mass in the tunnel area consisted of a series of crushed zones that are parallel to bedding stratification. The vertical distance between these zones varies between 50 m and 150 m. One of the crushed zones along the stratification separates two rock masses in different qualities. The rock mass below the zone is less fractured, massive and impermeable, and that above the zone is jointed. In addition to the bedding planes, there are two more distinct joint sets in the area. The orientation of one of the joint sets (J1) is about N55°–60°E/85°SE and that of another joint set (J2) is about N20°–25°W. The joint set J2 is almost vertical (Fig. 10).

After the failure of unlined tunnel occurred, the waterway system was drained and inspection was carried out. According to Bergh-Christensen (1975), during the inspection, it was observed that the cross joints nearby location *A* opened by about 3–4 cm between the tunnel sections *A* and *B* (Fig. 11). The opening in the joints clearly demonstrated the occurrence of hydraulic jacking.

The splitted joints crushed zones were studied in detail based on 3D maps and description of failure by Bergh-Christensen (1975). At the time of failure, the joints had opening from 10 cm to 50 cm at the location of heavy leakage in the surface. There were also moderate leakages where joints had about 1.5 cm-wide open cracks, which were completely washed out. During the excavation of pressure tunnel, the joint set (J1) was registered as dominant

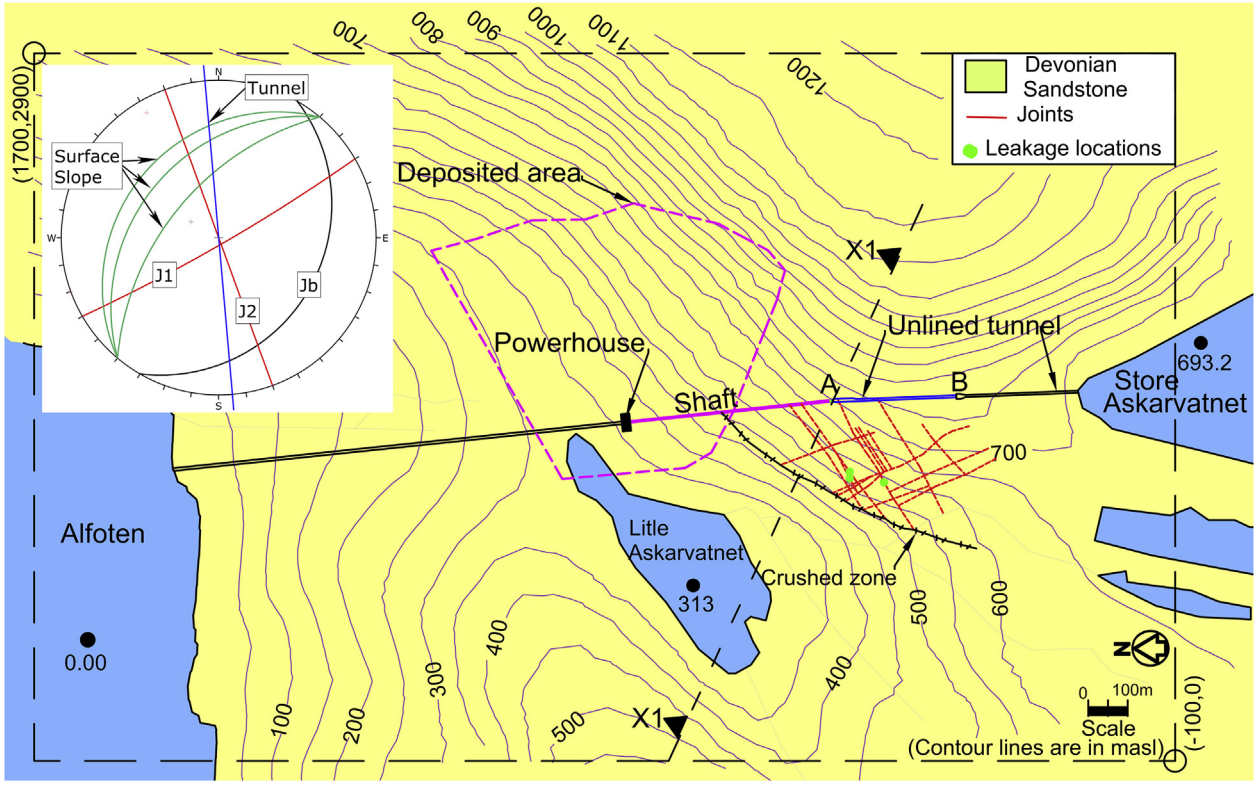

Fig. 10. Askara project area with rock type, crushed zone, joints (stereographic projection), and leakage locations.

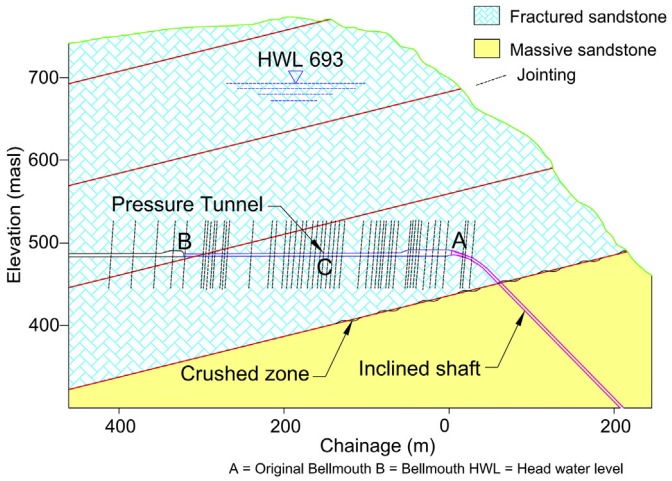

Fig. 11. Section through pressure tunnel of Askara power plant (Redrawn from Bergh-Christensen, 1975).

jointing system, which had 0.5–2 cm-wide opening filled with silt material. The joints were consistently becoming narrower, usually a few millimeter wide, beyond the chainage about 240 m from section *A* towards section *B* (Fig. 11). The narrower joints were filled with clay material. Similarly, another joint set (J2) in the outer part of the mountain was filled with silt and clay material.

4.4. Fossmark project

The waterway system of Fossmark project initially consisted of headrace tunnel, unlined pressure shaft, unlined pressure tunnel and steel-lined penstock tunnel connecting powerhouse located at the surface. The main rock type in the project is granitic gneiss. According to Garshol (1988), the rock mass of the project area consists of two distinct joint sets. The first joint set (J1) represents the zones of weakness and has strike of about NE–SW, dipping 20°–70° towards SE. Another joint set (J2) is striking NS and steeply dipping towards west. In Fig. 12, some of the joints are marked along the shaft and tunnel.

Garshol (1988) described the failure of unlined tunnel and shaft in detail. The failure was encountered both during excavation and test water filling. Water inflow into the tunnel was measured as 0.4 L/(s m) while excavating steel-lined and unlined pressure tunnels. Out of 15 marked joints along the unlined tunnel, nine joints were found out to be filled with silt and clay and the rest were observed without infilling material. The joint aperture is 0–5 cm wide and infilling thickness is from 1 cm to 2 cm. There are also some zones of weakness along the tunnel. Record indicates that two distinct zones of weakness were encountered during excavation of the shaft. The zones of weakness consisted of open joints from where water was lost while drilling. The marked joints and zones of weakness along the tunnel and shaft were considered as potential path for the leakage from unlined pressure shaft and tunnel.

The first test water filling was carried out up to 357 masl and gate was closed, since heavy leakage was noticed in the topography at the level of about 300 masl. After draining the water from the waterway system, inspection was carried out in the pressure tunnel, and it was observed that three joints were hydraulically deformed (failure locations are shown in Fig. 13). The infilling material of two joints was completely washed away and came down to the tunnel. Post injection grouting and shotcreting were carried out as a remedial measure. Thereafter, the second water filling was carried out up to the maximum level of 410 masl. The inspection after water drainage showed that one joint that followed from pressure tunnel to the shaft at 40 m from the shaft bottom was

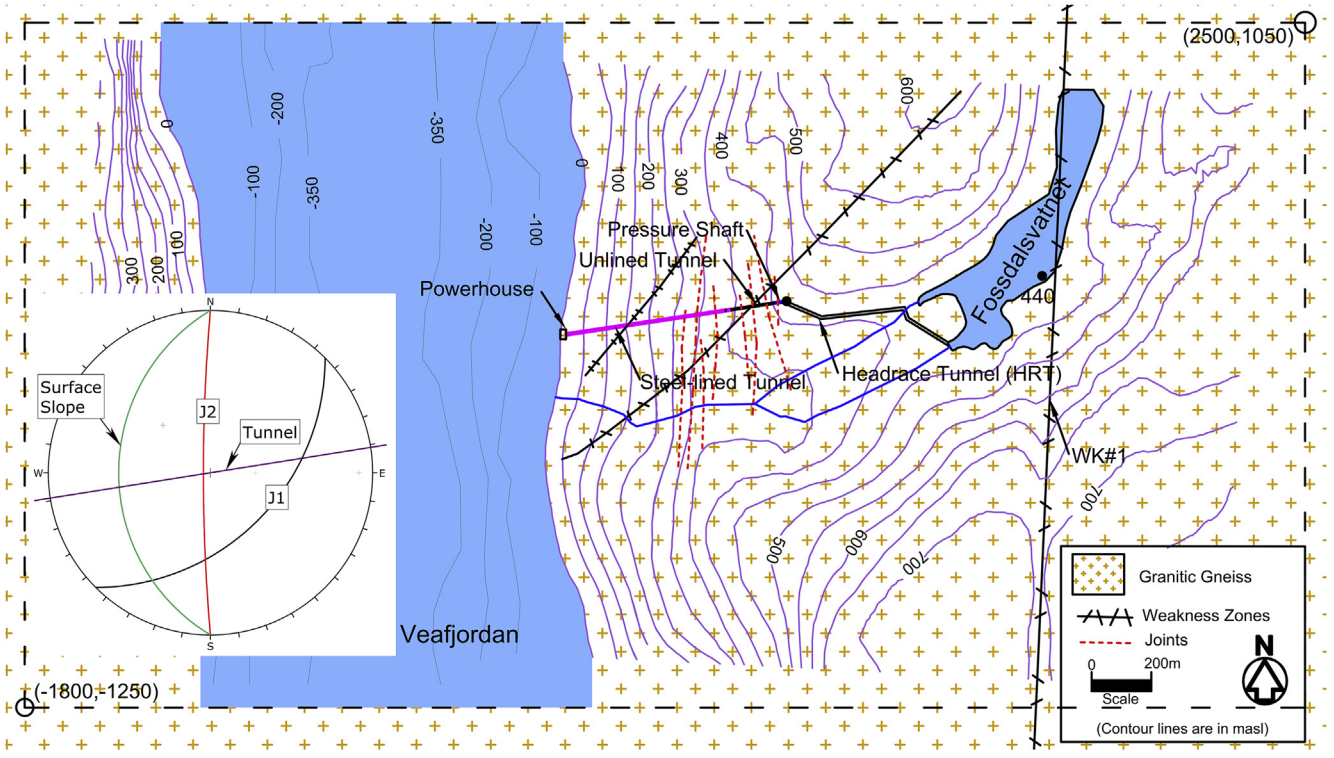

Fig. 12. Fossmark project area with various rock types, zones of weakness, and joints (stereographic projection).

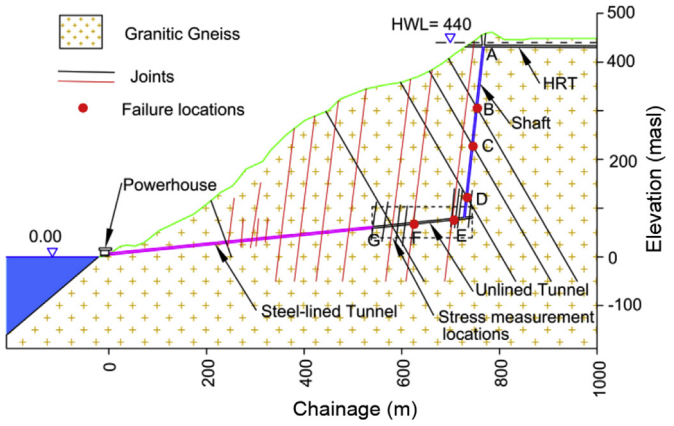

Fig. 13. Section through pressure shaft and tunnel of Fossmark project.

moved by 2–3 mm. In addition, several cubic meter rock fragments fell down at the bottom of the shaft. The inspection in the shaft was also carried out and it was observed that the rock fragments from the zones of weakness fell down. It was concluded that there existed cross communication between the joints in and nearby the shaft area. As a remedial measure, a comprehensive post grouting and shotcrete at the failure location in the shaft were applied.

During the last test water filling, which started with 2.75 m^3/min of water discharge, hydraulic splitting occurred at water level of 368 masl and water level in the shaft decreased even though the filling discharge was increased. The water level became stable at 330 masl with about 10 m^3/min of filling water discharge. At this water level, the overall leakage was estimated to be about 150 L/s (9 m^3/min). It was finally decided to use steel lining in both pressure shaft and tunnel. In order to examine the failure situation in terms of stress, both 3D-overcoring and hydraulic fracturings were employed close to the failure location of the unlined tunnel to find out the in situ stress state (Hanssen, 1997).

4.5. Naddevik project

The Naddevik project, one of the most successful unlined shaft projects, is located in south of Sogn and Fjordane on the west coast of Norway. As shown in Fig. 14, the main rock types of Naddevik area are dark gneiss and granitic gneiss (NGU, 2017). Dark gneiss is the basement rock where powerhouse is located and above which granitic gneiss is overlying.

According to Vik and Tunbridge (1986), a total of four 3D-overcoring and seven hydraulic fracturing stress measurement tests were carried out at this project to finalize the shaft alignment. The stress measurement locations are shown in both plan (Fig. 14) and profile (Fig. 15) of the project. Hydraulic fracturing was used in locations 1, 2 and 3 whereas 3D-overcoring was carried out at locations 2, 3, 4 and 5.

4.6. Nye Tyin project

Nye Tyin project is the highest head unlined tunnel project so far built worldwide. The maximum static head at the unlined tunnel of the project reaches 1047 m. The total length of unlined high pressure tunnel is about 11.5 km (Fig. 15).

The engineering geological aspect of the project area is described in Hydro (1998). The main rock types in the project area are dark gneiss as the basement rock, granitic gneiss, meta-arkose (sandstone), mica schist and phyllite (Fig. 15). According to SINTEF (2002), in situ stresses were measured at six locations along the powerhouse access tunnel, as indicated in Fig. 15 (location 1 starting from chainage 1100 m along access tunnel to location 6 at the penstock cone area). Both hydraulic fracturing (locations 1, 2, 4, 5 and 6) and 3D-overcoring (1, 3 and 6) techniques were applied to obtain the overview of the in situ stress state.

5. Input parameters for numerical analysis

The numerical modeling program FLAC^{3D} (Itasca, 2017a) is used for stress state analysis and UDEC (Itasca, 2017b) is used for fluid

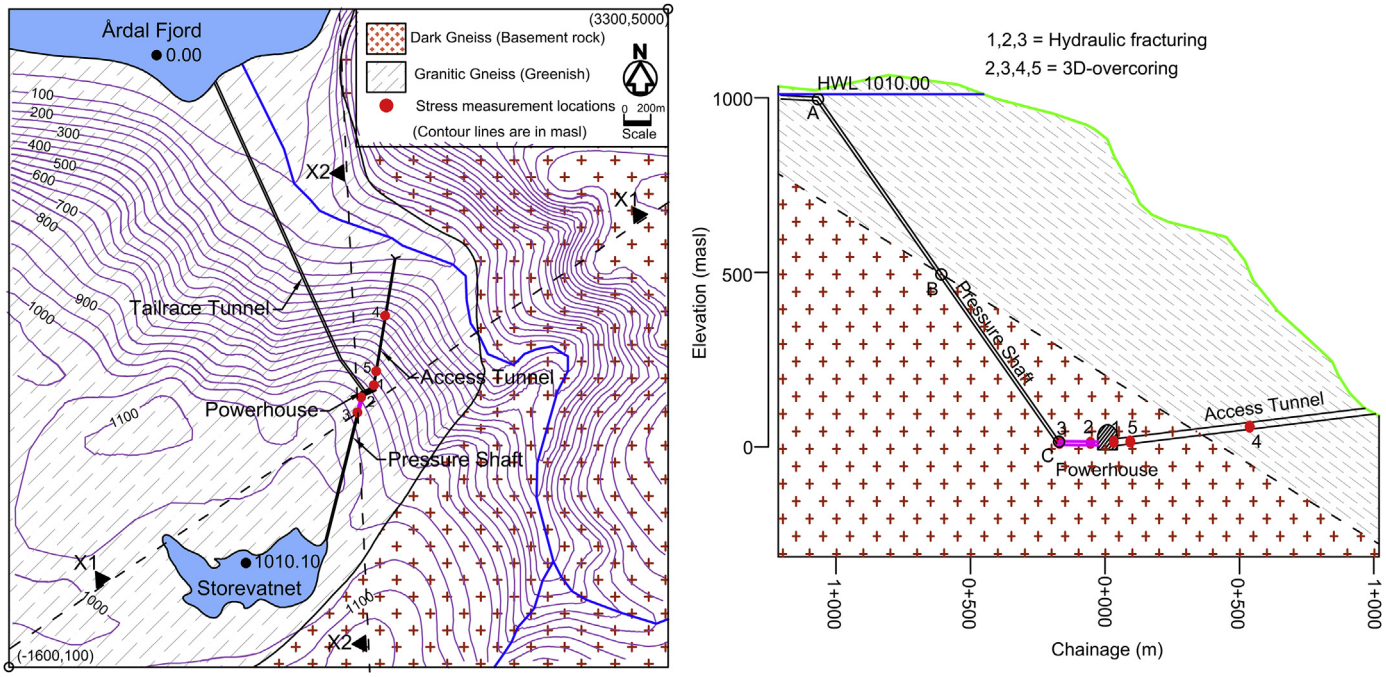

Fig. 14. Plan (left) and profile along the alignment (right) of Naddevik project.

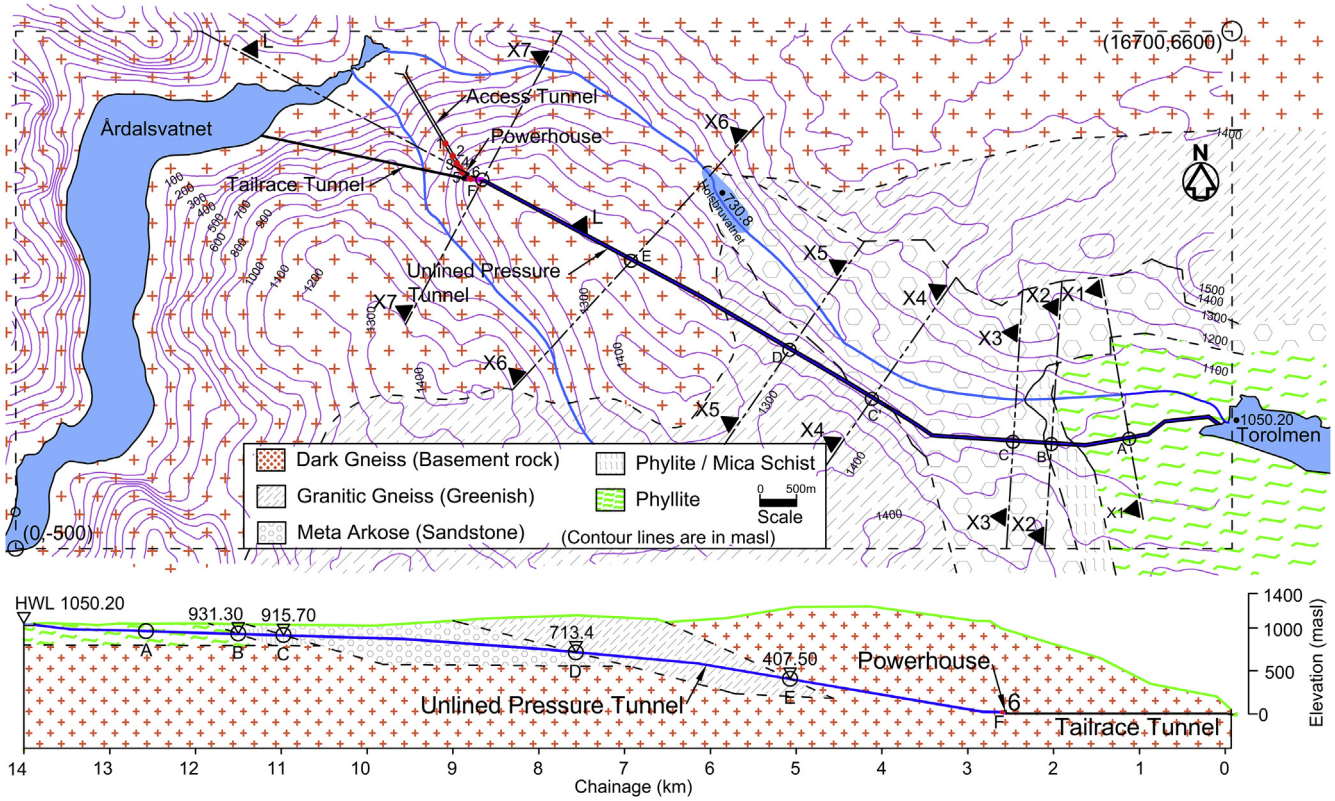

Fig. 15. Plan (upper) and profile (lower) along tunnel alignment of Nye Tyin project with stress measurement locations.

flow analysis in order to assess the occurrence of hydraulic jacking along the pre-existing joints. The input parameters required for the numerical analyses are quantified based on the detailed information collected from each project. The rock mass parameters, joint/interface parameters and in situ stress conditions are the most important input variables, which should be quantified for carrying out the numerical analyses.

5.1. Rock mass parameters

Rock mass parameters are required as input to define the quality of rock mass. Table 3 shows the mean values of rock mass parameters of different rock types. In Table 3, uniaxial compressive strength of intact rock (σ_{ci}), modulus of elasticity of intact rock (E_{ci}), Poisson's ratio (ν) and unit weight of the rock (γ) are the laboratory tested parameters of intact rock samples. Most of the laboratory tested values in Table 3 were collected from SINTEF (1998) excluding for unlined tunnels of Fossmark and Nye Tyin. The rock mass parameters of 'MS_weak' are assumed based on the description of rock mass conditions.

The bulk modulus (K) and shear modulus (G_{ci}) of intact rock in Table 3 are calculated using Eqs. (5) and (6), respectively, following Itasca (2017a):

$$K = \frac{E_{ci}}{3(1-2\nu)} \tag{5}$$

$$G_{ci} = \frac{E_{ci}}{2(1+\nu)} \tag{6}$$

The geological strength index (GSI) values are assumed 25 for zones of weakness and 90 for massive rock formations based on the engineering geological conditions of the particular case project. The disturbance factor (D) is assumed zero for the in situ condition (Hoek et al., 2002) and the material constant (m_i) is chosen from Hoek (2001) for the given rock types. The RocData software is used to estimate the rock mass deformation modulus (E_m). The rock mass shear modulus (G_m) is calculated using Eq. (6) where E_{ci} is replaced by E_m.

5.2. Joints/interface parameters

In the projects such as Byrte, Askara and Fossmark, fault/zones of weakness are modeled as plane of weakness in FLAC^{3D}. The planes are considered as the interface between two different rock formations and/or weakness/fault plane in the same or different rock formations. The joints are modeled in UDEC for fluid flow analysis and interfaces are modeled in FLAC^{3D} for stress state analysis. Joint parameters such as stiffness, aperture and permeability factor are important input parameters to UDEC model for fluid flow analysis and interface parameters such as stiffness and friction angle are important parameters to FLAC^{3D} (Itasca, 2017a, b).

5.2.1. Joint/interface stiffness

The joint stiffness is estimated by using the elastic properties of adjacent rock and rock mass. In this regard, Eqs. (7) and (8) are used to calculate joint normal and shear stiffnesses, respectively, as recommended by Itasca (2017a, b):

$$k_n = \frac{E_{ci}E_m}{s(E_{ci}-E_m)} \tag{7}$$

$$k_s = \frac{G_{ci}G_m}{s(G_{ci}-G_m)} \tag{8}$$

Table 3
Mechanical properties of different rock types of case projects.

Project	Rock type	σ_{ci} (MPa)	E_{ci} (GPa)	ν	G_{ci} (GPa)	K (GPa)	γ (kN/m^3)	GSI	D	m_i	E_m (GPa)	G_m (GPa)
Herlandsfoss	Mica schist[a]	56.1	31.1	0.14	13.6	14.5	27.7	60	0	12	16.2	7.1
	Hornblende schist[a]	80.4	61.2	0.23	24.8	37.9	30.5	75	0	26	49.9	20.3
	MS_Weak	16	20	0.14	8.8	9.3	27.7	25	0	12	1.2	0.5
Byrte	Granitic gneiss[a]	94.9	22.5	0.11	10.2	9.5	26.4	75	0	28	18.4	8.3
	Basalt[a]	186.8	69.5	0.31	26.6	59.7	27.7	75	0	25	56.7	21.7
Askara	Massive sandstone[a]	144.7	30.9	0.26	21.6	12.2	27.1	90	0	17	29.6	11.7
	Fractured sandstone[a]	144.7	30.9	0.26	21.6	12.2	27.1	70	0	15	22.6	9
Fossmark	Granitic gneiss[b]	188.8	43.5	0.13	19.3	19.3	26.4	80	0	32	38.3	17
Naddevik	Dark gneiss[a]	109.3	41.9	0.12	18.7	18.3	28.4					
	Granitic gneiss[a]	94.9	22.5	0.11	10.2	9.5	26.4					
Nye Tyin	Dark gneiss[c]	109.3	41.9	0.12	18.7	18.3	28.4					
	Granitic gneiss[a]	94.9	22.5	0.11	10.2	9.5	26.4					
	Meta arkose[d]	120.4	60.1	0.25	24.1	39.6	26.8					
	Phyllite[a]	40.5	39.8	0.25	15.9	26.3	27.5					

[a] SINTEF (1998).
[b] Hanssen (1997).
[c] SINTEF (2002).
[d] Laboratory tested value by authors.

where k_n is the joint normal stiffness, k_s is the joint shear stiffness, and s is the joint spacing. The stiffnesses of the rock and rock mass are already defined and estimated. Furthermore, Rocscience (2017) mentioned that the stiffnesses of fault or zones of weakness can be estimated from the properties of infilling material and thickness of the zone:

$$k_n = \frac{E_0}{t} \tag{9}$$

$$k_s = \frac{G_0}{t} \tag{10}$$

where E_0 and G_0 are the Young's modulus and shear modulus of infilling material, respectively, and t is the thickness of weakness/fault zone. The shear modulus of infilling material is calculated using Eq. (6) where E_{ci} is replaced by E_0 and ν is replaced by the Poisson's ratio of infilling material (ν_0).

5.2.2. Friction angle

Friction angle of the interface is also an important parameter to be estimated. Usually, it ranges from 15° to 30° in case of fault/zones of weakness (Barton, 1973). Friction angle of 25° is taken as the most likely value in the model.

5.2.3. Joint aperture and joint permeability factor

Itasca (2017b) gave the relationship for flow rate through the joints. The flow through joints depends upon contact hydraulic aperture (a) and joint permeability factor (k_j). The theoretical value of joint permeability factor is calculated by

$$k_j = \frac{1}{12\mu} \tag{11}$$

where μ is the dynamic viscosity of the water, which is equal to 1.306×10^{-3} Pa s at 10 °C (Kestin et al., 1978). The average temperature of water of about 10 °C is assumed for water tunnels of the case projects.

On the other hand, the contact hydraulic aperture is calculated by

$$a = a_0 + u_n \tag{12}$$

where a_0 is the joint aperture at zero normal stress, and u_n is the joint normal displacement (positive denoting opening). In UDEC model, a minimum value of aperture, a_{res}, is assumed for the aperture below which mechanical closure does not affect the contact permeability. Similarly, a maximum value, a_{max}, is also assumed as five times the a_{res}. The values for a_0, a_{res} and a_{max} are estimated based on the detailed joint information given for each project. Table 4 shows the estimated values of different joint/interface parameters.

5.3. Stress

Stress is another key input parameter in order to define the initial and boundary conditions in numerical models. Stress along Z-axis is mainly due to the vertical overburden of the rock mass. Part of the horizontal stress is due to vertical overburden, which is related to the Poisson's ratio.

In FLAC^{3D}, Y-axis is aligned to the north direction. The normal stresses along X- and Y-axis and corresponding shear stresses are calculated by resolving the maximum horizontal stress (σ_{Hmax}) and minimum horizontal stress (σ_{hmin}), as shown in Fig. 16.

The total stresses along Y- and X-axis are calculated by using Eqs. (13) and (14), respectively. Since the maximum horizontal stress makes an angle (θ) with Y-axis, there will be shear stresses in YZ and XZ faces as shown in Fig. 16 (the box shown in the figure has thickness along Z-axis). The shear stresses will have the same magnitude in both faces and are estimated by using Eq. (15). The shear stresses shown in Fig. 16 are negative.

$$\sigma_{yy} = \sigma_{Hmax} \cos^2\theta + \sigma_{hmin} \sin^2\theta \tag{13}$$

$$\sigma_{xx} = \sigma_{Hmax} \sin^2\theta + \sigma_{hmin} \cos^2\theta \tag{14}$$

$$\sigma_{xy} = \sigma_{yx} = \frac{\sigma_{Hmax} - \sigma_{hmin}}{2} \sin(2\theta) \tag{15}$$

Since there was no stress measurement in Herlandsfoss, Byrte and Askara projects, measured stress data from nearby locations (as shown in Fig. 2) are taken as the reference values. The principal horizontal stresses at the measured locations are resolved along X- and Y-axis. Then the horizontal stress due to vertical overburden is subtracted from each resolved stress, which gives the stress due to tectonics along X- and Y-axis, respectively. These tectonic stresses along X- and Y-axis are transferred to initialize the horizontal stresses in 3D model of each project area. On the other hand, the

Table 4
Input parameters for joints and interfaces.

Project	Joints/zone of weakness	E_{ci} (GPa)	G_{ci} (GPa)	E_m (GPa)	G_m (GPa)	E_0 (GPa)	ν_0	G_0 (GPa)	s or t (m)	k_n (GPa)	k_s (GPa)	a_0 (mm)	a_{res} (mm)	Remarks
Herlandsfoss	Jf	20	8.8	1.2	0.5				5.6	0.23	0.095	1	0.5	Joint
	2	20	8.8	1.2	0.5				11.2	0.11	0.047	3	1	Joint
	3	20	8.8	1.2	0.5				11.2	0.11	0.047	3	1	Joint
	4	20	8.8	1.2	0.5				11.2	0.11	0.047	3	1	Joint
	5	61.2	24.8	49.9	20.3				18.1	15	6.2	0.1	0.05	Joint
	6	61.2	24.8	49.9	20.3				18.1	15	6.2	0.1	0.05	Joint
Byrte	Joint#a1	22.5	10.2	18.4	8.3				30	3.4	1.5	3	1	Joint
	Joint#a2	22.5	10.2	18.4	8.3				20	5	2.2	3	1	Joint
	Joint#a3	22.5	10.2	18.4	8.3				10	10	4.5	3	1	Joint
	Joint#b	22.5	10.2	18.4	8.3				35	2.9	1.3	10	5	Joint
	WK#1					0.4	0.1	0.2	3	0.13	0.061	10	5	Zone of weakness
	WK#2					0.4	0.1	0.2	3	0.13	0.061			Zone of weakness
	Byrte_Fault					0.4	0.1	0.2	20	0.02	0.0091	3	1	Fault
Askara	Jb	30.9	12.2	22.6	9				100	0.85	0.34	5	1	Sliding zone/Joint
	J1	30.9	12.2	22.6	9				10	8.5	3.4	5	1	Joint
Fossmark	WK#1					0.4	0.1	0.2	20	0.04	0.018			Zone of weakness
	J1					0.4	0.1	0.2	0.5	0.8	0.36	5	1	Joints/zones of weakness
	J2	43.5	19.3	38.3	17				20	16	7.1	5	1	Joint

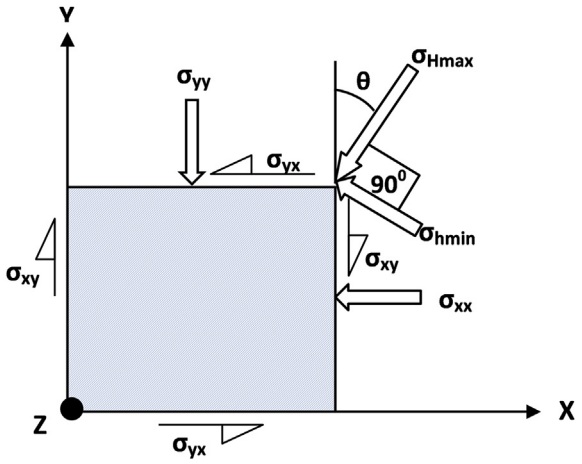

Fig. 16. Resolving horizontal stresses in *X* and *Y* directions.

shear stresses remain unchanged. The input stresses to FLAC^{3D} model of three projects are shown in Table 5.

For other three projects, i.e. Fossmark, Naddevik and Nye Tyin, the magnitude and orientation of maximum and minimum horizontal stresses are iterated in FLAC^{3D} to match the principal stresses measured by 3D-overcoring technique at respective locations. The orientation of maximum horizontal stress is also compared with the regional tectonic stress regime. In addition, the minor principal stress measured by hydraulic fracturing is also compared with the model result. The measured stress values, which are used for validation purpose, are given in Table 6.

6. Numerical analysis

As explained earlier, the minor principal stress is the key parameter for the design of unlined pressure shafts and tunnels. FLAC^{3D} model is used to analyze the stress state (especially the minor principal stress) for all six projects, i.e. Herlandsfoss, Byrte, Askara, Fossmark, Naddevik and Nye Tyin. In addition, hydraulic jacking and leakage assessment on the failed cases of pressure tunnels and shafts of Herlandsfoss, Byrte, Askara and Fossmark projects are carried out using UDEC model.

6.1. Stress state analysis

The stress state analysis is carried out in order to quantify the minor principal stress at the location of unlined shaft and tunnel. In FLAC^{3D}, a 3D geometry of the selected area for each project is created incorporating the surface topography, as shown in Fig. 17. After the geometry is defined, 3D tetrahedral volume grids of different sizes are created. The sizes of the grids are finer nearby the location of tunnel and shaft. In addition to the 3D geometry and grids, the model is supplemented with the defined interfaces in Byrte, Askara and Fossmark projects according to Figs. 8, 10 and 12, respectively. The mechanical properties of each rock type (Table 3) are assigned in the model. The mechanical properties of interfaces (Table 4) are also assigned in the model for Byrte, Askora and Fossmark projects where hydraulic jacking occurs. First, the model is run to initialize the gravity-induced vertical and horizontal stresses. Once the model is converged to the equilibrium within prescribed limit of unbalanced force, the total stresses including tectonic stresses are initialized and the model has been run once again until the second equilibrium state is reached. After that, the model is considered to be ready for in situ stress evaluation.

In Herlandsfoss project, the failed location having highly schistose mica schist band near the boundary with hornblende schist is considered to be very weak rock mass (MS_Weak), as indicated in Fig. 17a. Fig. 18 shows the minor principal stress along the tunnel alignment at Herlandsfoss project. As seen in Fig. 18, there is de-stressing in the in MS_Weak zone in comparison to the pressure tunnel area consisting of relatively good quality mica schist (MS) and hornblende schist (HS). Fig. 18b shows the influence of stiffness of weak mica schist (MS-Weak), which indicates that the lower the stiffness of the rock material is, the higher the de-stressing will be.

In Byrte project, the zones of weakness are also modeled as interfaces (Fig. 17b). The influence of zones of weakness on the stress state is clearly seen in Fig. 19a. An analysis is carried out to see whether failure is initiated at point *C* (Fig. 19) once the maximum water level reaches about 725 masl with the hydrostatic head of 195 m. Since a hydraulic jacking occurs at point *C*, it is logical to assume that the minor principal stress at this point is close to the hydrostatic pressure created by the maximum water level of 725 masl. It is observed in FLAC^{3D} model that the stress state at the rock mass 'G_Gneiss2' seems sensitive to the change in stiffness of the zones of weakness and the Byrte fault. Hence, the elastic modulus (E_0) of the rock material in the zone of weakness (the

Table 5
Calculation of input stresses to FLAC^{3D} model.

Project	γ (kN/m^3)	ν	Stress measurement					Input stresses (only tectonic) (MPa)		
			Location	h (m)	σ_{Hmax} (MPa)	σ_{Hmin} (MPa)	σ_{Hmax} direction (°)	σ_{xx}	σ_{yy}	σ_{xy}
Herlandsfoss	29.1	0.2	L-1	75	7	3	N35°E	3.8	5.1	1.88
Byrte	26.4	0.11	L-2	400	22.7	5.5	N90°E	21.4	4.2	0
Askora	27.1	0.26	L-3	20	17	10	N90°E	16.8	9.8	0

Table 6
Measured stresses at different locations of Fossmark, Naddevik and Nye Tyin projects.

Project	Location	h (m)	Major principal stress, σ_1			Intermediate principal stress, σ_2			Minor principal stress, σ_3			Remarks
			Mean (MPa)	SD (MPa)	Trend (°)/Plunge (°)	Mean (MPa)	SD (MPa)	Trend (°)/Plunge (°)	Mean (MPa)	SD (MPa)	Trend (°)/Plunge (°)	
Fossmark[a]	Unlined	275	7.1	3.4	350/35	5.5	1.5	198/52	0.6	4.4	089/13	OC
	tunnel	275							2.7	0.8		HF
Naddevik[b]	1	880							18			HF
	2	900	26.3		282/52	18.9		140/45	12.4		032/25	OC
	2	900							12.7			HF
	3	930	25		076/40	19.6		232/60	16.8		340/22	OC
	3	930							14.2			HF
	4	450	16.1		180/55	12.3		280/18	4.9		027/50	OC
	5	750	20.9		304/65	14.6		144/30	12.2		047/15	OC
Nye Tyin[c]	1	700	15.2	1.88	031/26	9.2	1	292/17	5.2	2	173/58	OC
	1								11.2	1.7		HS
	2								17.1	3.7		HS
	3	950	31.2	2.1	349/03	25.8	2.7	087/66	19.9	1.5	258/24	OC
	4								12.4	2.2		HS
	5								17	6.6		HS
	6	1000	49.5	4.6	013/13	21.1	2.1	262/58	15.9	4.4	110/29	OC
	6								26	4.1		HS

OC = 3D-overcoring; HF = Hydraulic fracturing; HS = Hydraulic splitting; SD = Standard deviation.
[a] Hanssen (1997).
[b] Vik and Tunbridge (1986).
[c] SINTEF (2002).

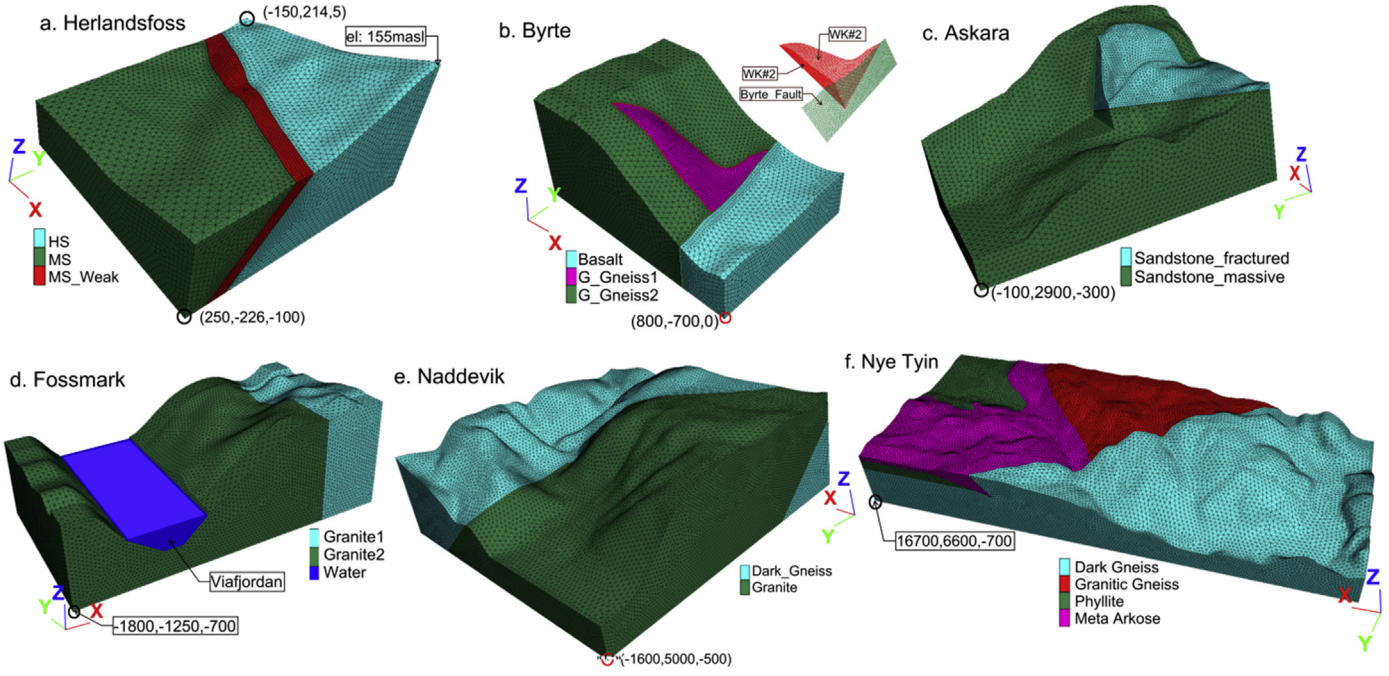

Fig. 17. 3D geometry of different project areas (HS: Hornblende schist; MS: Mica schist; G_Gneiss1 & G_Gneiss2: Granitic gneiss).

same is assumed for both WK#1 and WK#2 and for Byrte fault) is varied between 0.2 GPa and 1 GPa to assess the sensitivity and the corresponding minor principal stress at point C is identified (Fig. 19b). As seen in the figure, the minor principal stress becomes equal to the water pressure at point C with E_0 value of about 0.4 GPa. Hence, this value of E_0 is used to evaluate the final stress state along Byrte pressure shaft and tunnel system (Fig. 19c).

In Askora project, the surface topography has slopes in both north and west directions at the location of unlined tunnel. In addition to the rock mass, the crushed zone is also modeled in

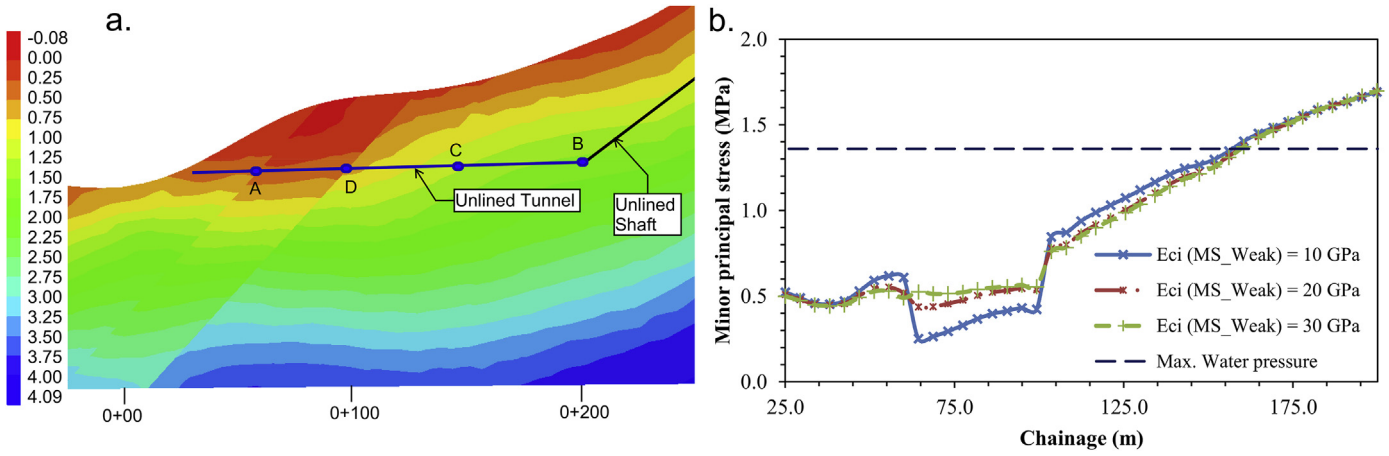

Fig. 18. (a) Minor principal stress (MPa) along the tunnel alignment (E_{ci} of MS_Weak is 20 GPa); (b) Minor principal stress at different E_{ci} values in Herlandsfoss project.

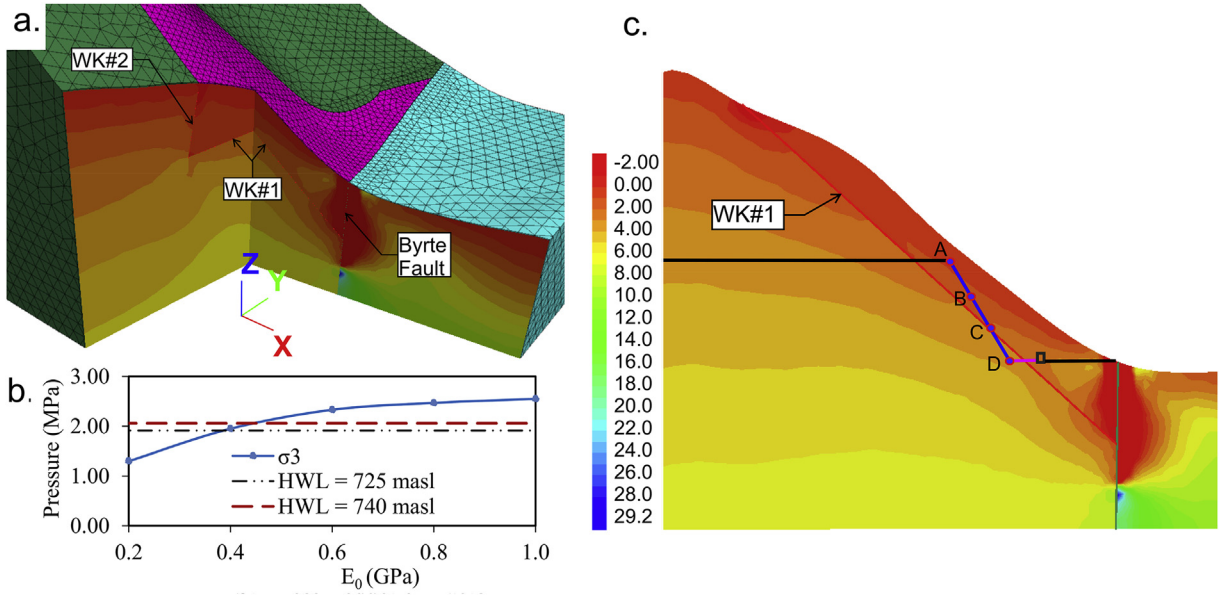

Fig. 19. (a) Influence of zones of weakness on stress state; (b) Minor principal stress at point *C* at different values of E_0; (c) Minor principal stress (MPa) along tunnel and shaft alignment of Byrte project.

FLAC^{3D} (Fig. 17c). The influences of both the slopes and the crushed zone on the stress state of the area are shown in Fig. 20a and b, respectively. The magnitude of the minor principal stress along the tunnel and shaft alignment shown in Fig. 20b is further used for the evaluation of stress requirement for the unlined tunnel at locations *A*, *B* and *C*.

In case of Fossmark project, the stiffness of the zone of weakness is assumed, as indicated in Table 4. The magnitude and orientation of the maximum and minimum horizontal stresses are assumed based on the stress regime of nearby area and the model is run for each stress input in order to match the measured stress. It is found that the maximum horizontal stress of about 9 MPa (only tectonic stress) with orientation of about N15°E and the minimum horizontal stress of about 5 MPa (only tectonic) gives good match with the measured stress at Fossmark project (Table 6).

Fig. 21 shows the magnitude of the minor principal stress along the shaft and tunnel alignment of Fossmark project. The model is run for two different conditions. At first, the model is run with the zone of weakness and the corresponding stresses are converged to measured stresses. The minor principal stress indicated in Fig. 21a is accounted as the final result for the analysis of stress state along the shaft and tunnel alignment of Fossmark project. The model is once again run without incorporating zone of weakness (Fig. 21b) to observe the influence of the zone of weakness on the stress regime. Fig. 21a and b clearly indicates that there is a considerable influence of zone of weakness on the stress state.

In Naddevik project, the 3D stresses measured at different locations are used to compare the result from FLAC^{3D}. The locations 2 and 3 are chosen to be decisive for the comparison, because there is less influence by the valley slope on the stress development since they are located in the innermost locations from the slope topography. In FLAC^{3D}, magnitude of the principal stresses at these locations is converged to the corresponding measured values when the maximum horizontal stress (only tectonic) of 21 MPa is applied along N125°E. The corresponding minimum horizontal stress is 13 MPa. The model is then considered to be ready for the final stress

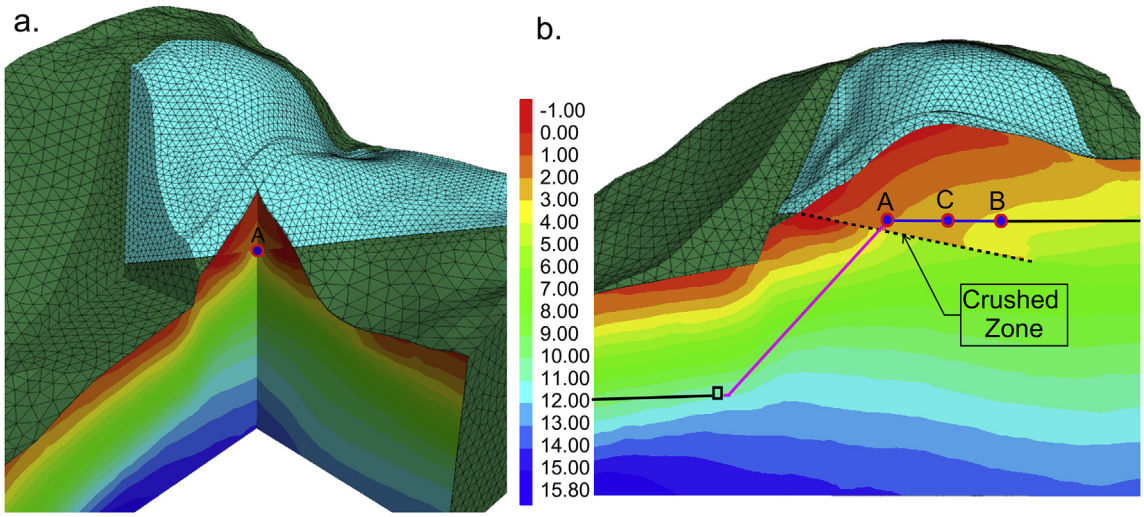

Fig. 20. (a) 3D influence of valley side slopes and sliding zone on stress state; (b) Minor principal stress (MPa) along tunnel and shaft alignment of Askora project.

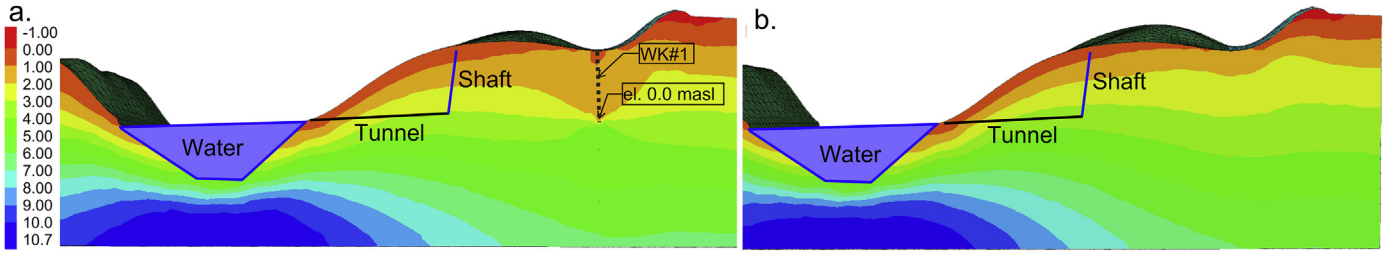

Fig. 21. Minor principal stress (MPa) along tunnel and shaft alignment of Fossmark project (a) with zone of weakness and (b) without zone of weakness.

state evaluation. Fig. 22a shows the final result of magnitude of the minor principal stress along the alignment of Naddevik project, and Fig. 22b shows the comparison between the model result and the minor principal stress measured at different locations.

In Nye Tyin project, the result obtained from FLAC^{3D} is compared with the measured stress magnitudes at different locations, and location 3 is found to be representative with respect to the orientation of the maximum horizontal stress as explained by Fejerskov et al. (2000). Fig. 23a shows the final result of magnitude of the minor principal stress along the tunnel alignment of Nye Tyin project. Fig. 23b shows the comparison between the minor principal stress obtained from the model and measured at different locations.

6.2. Fluid flow analysis

The fluid flow analysis through the joints is carried out in order to evaluate the possibility of hydraulic jacking and leakage. In this regard, 2D geometries along the pressure tunnel/shaft alignment of Herlandsfoss, Byrte, Askara and Fossmark are created in UDEC program and the coordinates of the geometries are in accordance with Figs. 7, 9, 11 and 13, respectively. The rock mass and representative joint systems are also modeled in the geometry (Fig. 24). The assigned properties of rock mass and joints shown in Tables 3 and 4, respectively, are used as input variables. The boundary stress along *X*-axis is assigned based on the values from FLAC^{3D}, whereas the stress along *Y*-axis is generated by gravity itself and the bottom

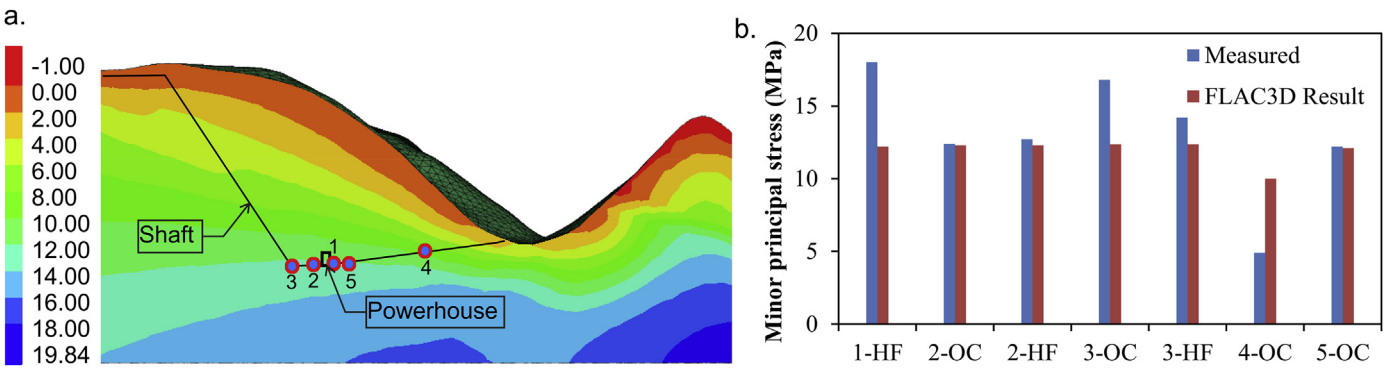

Fig. 22. (a) Minor principal stress (MPa) along shaft alignment, and (b) Comparison between measured values and FLAC^{3D} result at stress measurement locations of Naddevik project.

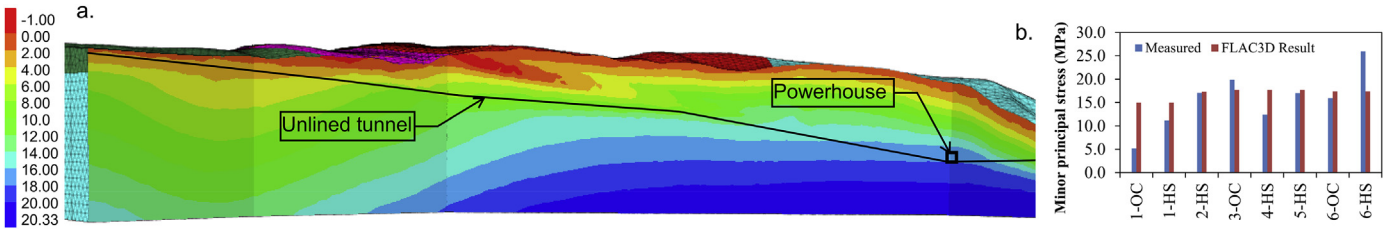

Fig. 23. (a) Minor principal stress (MPa) along tunnel alignment, and (b) Comparison between measured values and FLAC^{3D} result at stress measurement locations of Nye Tyin project.

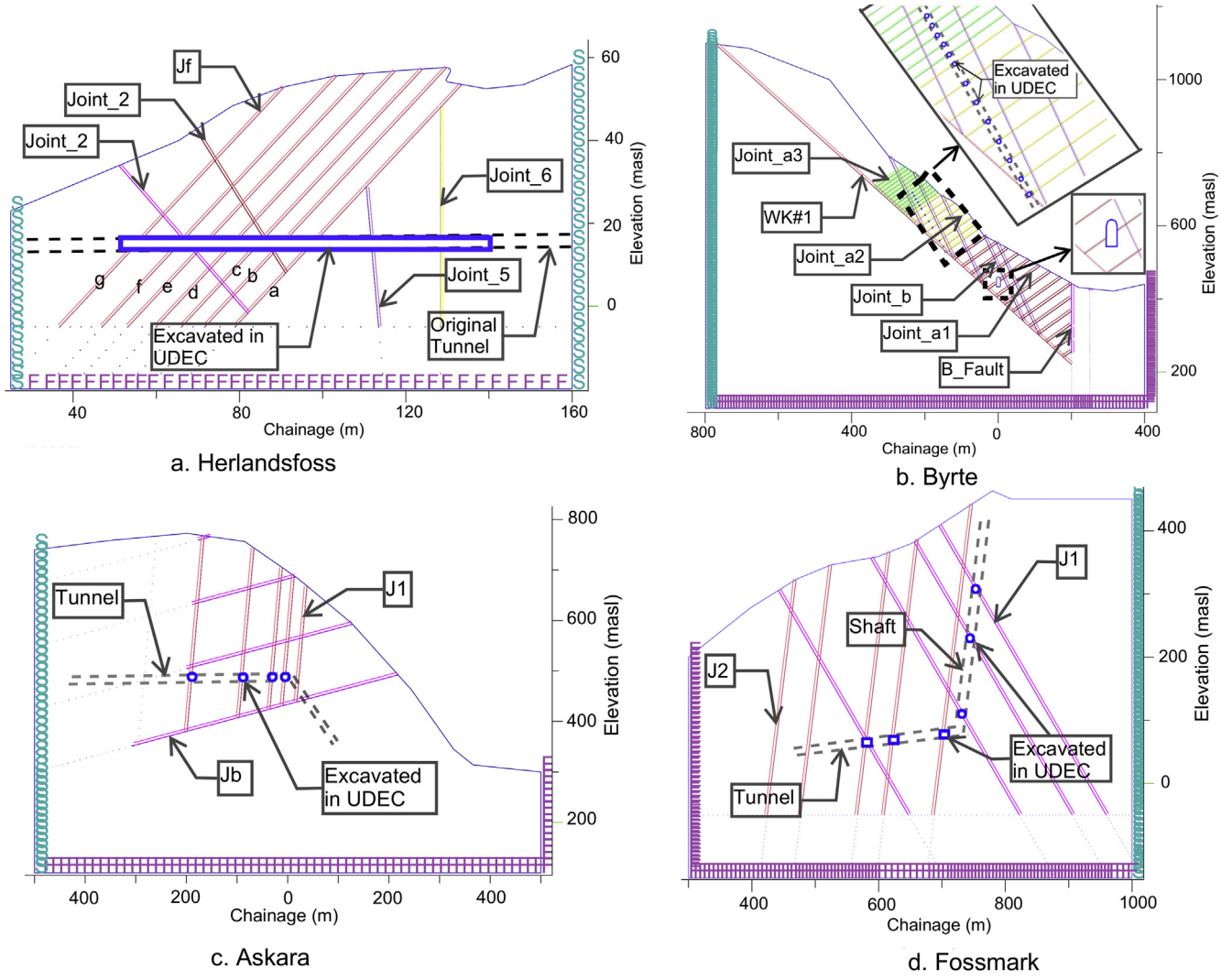

Fig. 24. 2D geometry in UDEC with rock types and representative joints of the selected projects.

of the model is fixed against displacement. All the boundaries except the top are made impermeable against fluid flow. The model is run for incompressible fluid flow through the joints.

The UDEC model is run until it comes to the mechanical equilibrium after the geometry has been created and boundary conditions have been applied. The tunnel/shaft is excavated at the selected locations only as shown in Fig. 24. The excavation locations are selected keeping in mind that all the representative joints along the alignment can be assigned with designed water flow without violating the model equilibrium. If the whole tunnel/shaft is excavated in UDEC, it is difficult to generate the required amount of fluid pressure especially in case of inclined or vertical alignment. Fluid flow at the excavated locations (Fig. 24) is then assigned and the maximum pressure is limited to the maximum hydrostatic head at the respective locations. The model is once again run until the total fluid flow time is reached. Domain pore pressure developed after the end of total fluid flow time is shown in Fig. 25. Furthermore, as shown in Fig. 25, different locations are selected to track the pore pressure built-up along the joints. The locations are chosen nearby the tunnel/shaft and at the surface topography in order to assess potential hydraulic jacking and their potential leakage.

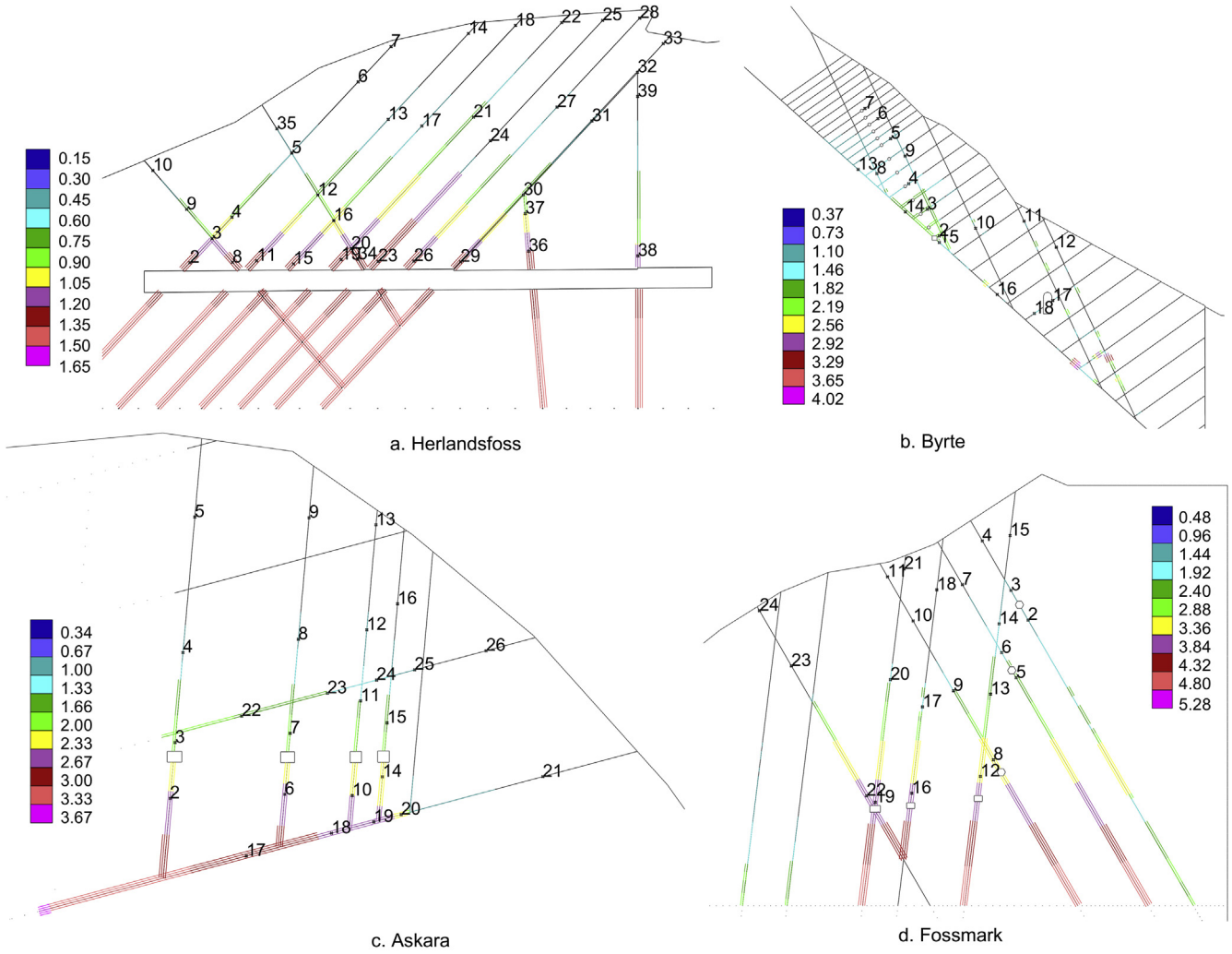

Fig. 25. Domain pore pressure (MPa) and tracking locations.

7. Analysis results

In the following, the results of the analysis are summarized. The results include assessment on the overall engineering geological conditions of the failed cases, the minor principal stress state at different locations of unlined tunnels and shafts, and assessment of hydraulic jacking and leakage through the pre-existing joints.

7.1. Engineering geological assessment

Engineering geological assessment and comparison of the failed cases are made based on geological formations, rock types, jointing conditions, faulting, severity of leakage and failure condition experienced by each case. Even though all seven failure cases, which experienced partial collapse after first water filling, are situated in different geological formations, there exists commonness regarding jointing conditions. The geological formations, rock types, jointing and infilling conditions, and nearby faults are highlighted in Table 7.

As seen in Table 7, all the cases have two major joint sets with one of the joint set steeply dipping and unfavorably orientated. In addition, the joints are filled with silt and clay mineral coating, which could be washed away. Open and permeable joints formed leakage paths, making it easy for the pressure built-up, and increased hydraulic jacking potential. The nearby faults facilitate this process further. Therefore, the real challenge for the successful unlined pressure tunnels and shafts is to avoid potential hydraulic jacking, which leads to excessive leakage and potential tunnel collapse.

7.2. Minor principal stress

The minor principal stresses obtained from FLAC^{3D} model at different locations of all selected projects are shown in Fig. 26. The factor of safety (FoS_3) is calculated by dividing the minor principal stress by water pressure (Fig. 26). FoS_3 is more than one in most of the locations except the locations Hf-A, Hf-D, Br-C, As-A, Fo-B, Fo-C, Fo-D, Fo-E, Fo-F and Fo-G. The figure also shows the factors of safety calculated using Norwegian design criterion discussed previously (FoS_1 and FoS_2). In general, there is an agreement between different factors of safety in terms of whether they are more or less than one excluding Hf-C and Br-D where FoS_1 and FoS_2 are less than one and FoS_3 is more than one. It is highlighted here that no failure is experienced in these locations. In the locations such as As-A, Fo-B, Fo-C, Fo-D, Fo-E and Fo-F (except Fo-G), the results of FoS_3 agree with the actual incident that had occurred during test water filling and initial phase of the project operation.

In the locations such as Br-A and Br-B, the calculated factor of safety using all three approaches is higher than one. However, this does not agree with the actual conditions because failure occurred

Table 7
Summary of the geology, rock types, jointing, joint filling conditions, faulting, leakage and failure description.

Project	Geology and rock types	Jointing	Joint infilling	Fault and zones of weakness	Leakage (L/s)	Specific leakage (L/(min m))	Failure condition
Herlandsfoss	Cambro Silurian hornblende schist and mica schist	Two joint sets: intersecting joints consisting foliation joint and cross joints	Mica schist is highly schistose and rich in chlorite and muscovite at the failure location	Failure occurred through the band of highly schistose rock mass representing a zone of weakness	300	419	Hydraulic jacking and lifting of rock mass occurred
Skar	Precambrian granitic gneiss	Foliation joints and random joints in all directions	Schistosity formation along the foliation joint and occasional hornblende mineral coating	No nearby fault exists	100	10	Hydraulic jacking occurred
Svelgen	Devonian sandstone	Gently dipping bedding joints and cross joints dipping almost perpendicular to the tunnel alignment intersect	Altered joints either open or filled with silt and clay	No nearby fault exists	70	3	Minor leakage and no hydraulic splitting
Byrte	Precambrian granitic gneiss	Several systems of joints with some steeply dipping joints	Joints are silt and clay filled	Long persisting clay filled zone of weakness almost parallel to the valley side slope. Byrte fault is located at about 200 m downstream from powerhouse	1000	194	Hydraulic jacking occurred through zone of weakness and movement of rock mass outside of the zones of weakness
Askara	Devonian sandstone	Two distinct joint sets consisting of foliation and steeply dipping cross joints	Cross joints have opening of 5–20 mm and are filled with silt and clay	A crushed zone separates fractured rock mass with massive one	1000	185	Hydraulic jacking occurred and a joint at the end of unlined tunnel was opened by about 3–4 cm and extended up to the ground surface
Bjerka	Cambro-Silurian granitic gneiss	Two joint sets: widely spaced foliation joints and steeply dipping cross joints	The cross joints that are perpendicular to the tunnel alignment have 1–10 mm opening and filled with silt and clay	No fault zone	1200	900	Hydraulic jacking occurred in a joint that opened approximately 2 cm in walls and 5.3 cm in the floor at the end of unlined tunnel
Fossmark	Precambrian granitic gneiss	Two distinct joint sets: Steeply dipping joint set striking parallel to valley side and other joint set representing the zones of weakness	Some joints along pressure tunnel are filled with silt and clay and some are without filling. The joints have opening from 0 to 5 cm and infilling from 1 cm to 2 cm	Zones of weakness in shaft and tunnel area dipping towards the mountain. A distinct zone of weakness is found across the reservoir lake striking parallel to the fjord valley	150	12	Hydraulic jacking occurred in three joints along the pressure tunnel. The infilling of two joints was completely washed away into the tunnel. Rock mass failed in two zones of weakness in the shaft

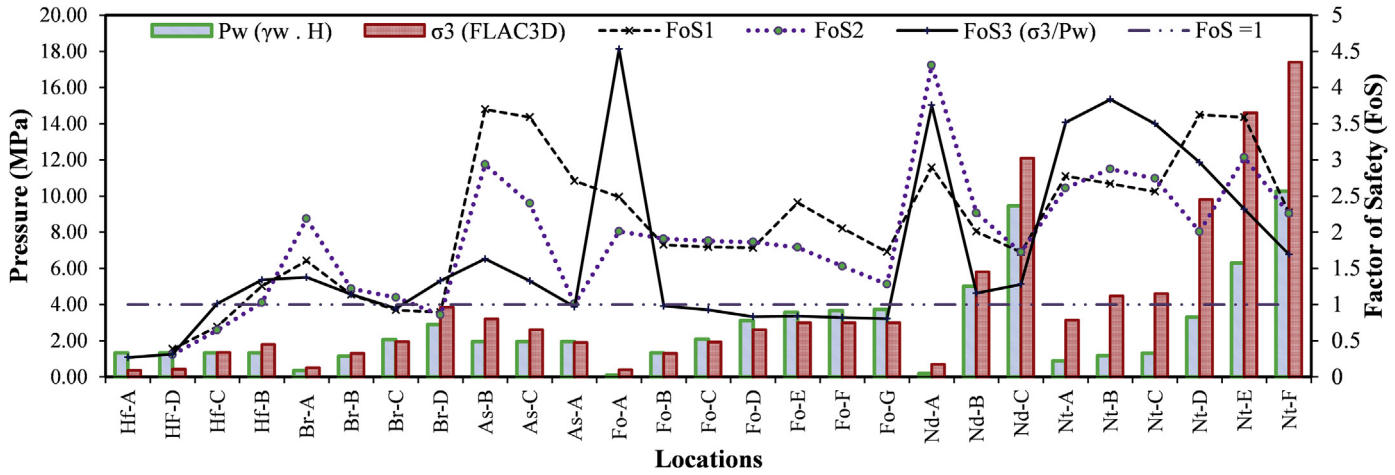

Fig. 26. Minor principal stress (σ_3) from FLAC^{3D} model, water pressure (P_w), and factor of safety at different locations of the projects.

in these locations during test water filling. The reason behind the failure may have been attributed to the situation that the failure initiated from the lower part of shaft, which initiated deformation along the joints that are subparallel to the shaft alignment and extended to the surface. Further, the fluid flow analysis would be helpful to assess hydraulic jacking and leakage in such condition. On the other hand, the minor principal stresses along the unlined shaft and tunnel of Naddevik and Nye Tyin projects satisfy the required factor of safety.

7.3. Hydraulic jacking and leakage assessment

An assessment of occurrence of hydraulic jacking and leakage is carried out in all four projects (Herlandsfoss, Byrte, Askara and Fossmark). Fig. 27 shows the pore pressure built-up at different locations of Herlandsfoss project over the specified fluid flow time in the UDEC at different joints (joints a, c, e, g, 2, 4, 5 and 6). There is rise in the pressure built-up at the beginning of fluid flow time in all the locations. After a while, the pressure reached to the maximum hydrostatic head in the locations nearby tunnel (locations 2, 8, 15, 23, 26, 29 and 34) and remained constant until the total flow time. However, in most of the other locations, the pressure drops when it reaches the corresponding hydrostatic head or sometimes even before. This condition shows the sign of hydraulic jacking of joints at these locations. More interestingly, there is pressure built-up and eventually hydraulic jacking in the locations nearby the surface topography, which indicates the possibility of leakage through the joints all the way to the surface.

In Byrte project, there is pressure built-up in almost all the locations (Fig. 28). The pressure starts to rise after certain fluid flow time and reaches its maximum in the locations nearby the shaft (locations 2, 3, 4, 5, 6 and 7) and indication of hydraulic jacking can be seen in locations 2, 3, 5 and 6. The pressure starts to rise up in the location nearby the powerhouse (location 18) along joint a1. This pressure built-up and hydraulic jacking at location 18 clearly indicate water leakage into the powerhouse cavern experienced during operation. Similarly, the locations along joint b also experienced pressure built-up and hydraulic jacking. The pressure built-up at locations nearby the surface topography (locations 11 and 12) clearly indicates the possibility for water leakage at surface. There is also pressure built-up and hydraulic jacking at locations along the zone of weakness (locations 13, 14, 15 and 16), as indicated in Fig. 28d.

Fig. 29 shows the domain pressure at different locations of Askara project. There is pressure built-up in almost all the locations except locations 5, 9 and 13 that are located well above the

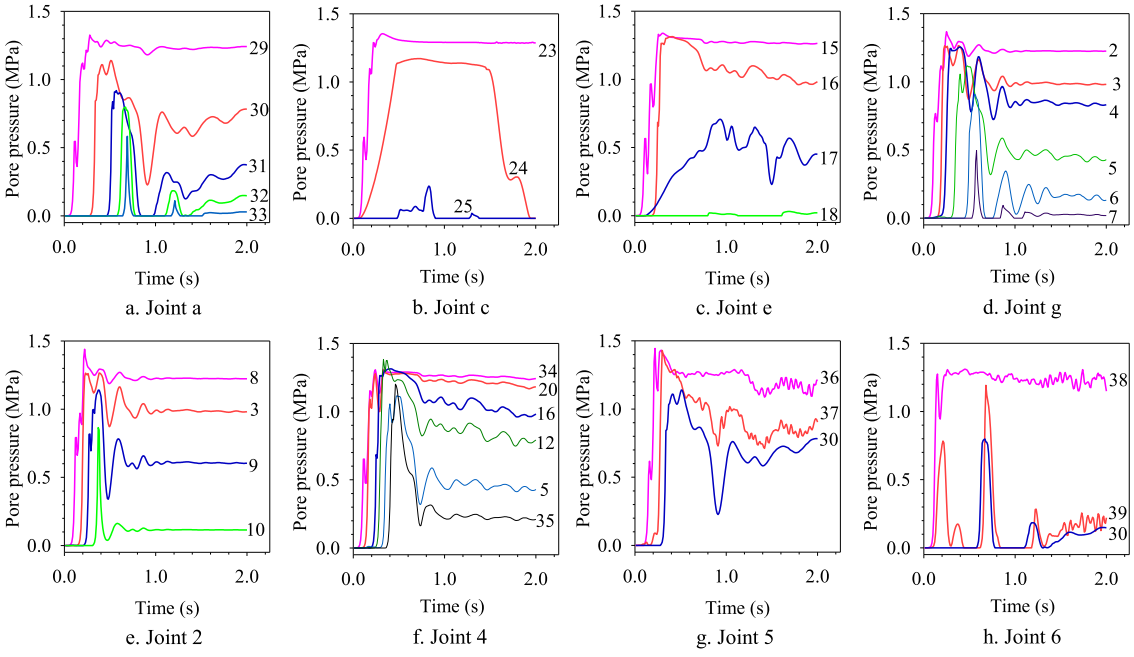

Fig. 27. Domain pore pressure vs. fluid flow time along different joints of Herlandsfoss project.

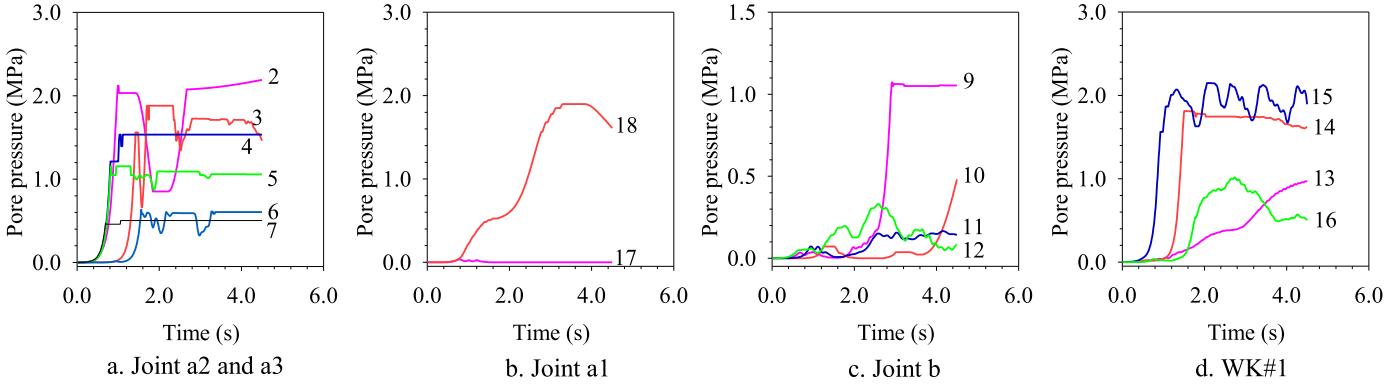

Fig. 28. Domain pore pressure vs. fluid flow time along different joints of Byrte project.

maximum water level. The hydraulic jacking observed in locations 16, 21 and 26 clearly indicates the leakage through the corresponding joints. Fig. 29 also shows that the hydraulic jacking occurs in locations 11, 12, 18, 19, 20, 23, 24 and 25. However, the extent of jacking is different from location to location.

In Fossmark project, the locations are chosen along both joints J1 and J2. There is pressure built-up in almost all the locations considered (Fig. 30). The pressure increases after the certain fluid flow time in all the locations and eventually reaches its maximum in the locations nearby shaft and tunnel. There is clear indication of hydraulic jacking at location 7, which is near the surface topography. The pressure vs. flow time diagram does not clearly indicate the hydraulic jacking of joints at the locations nearby shaft and tunnel. However, the pressure built-up at these locations confirms that the fluid flows through the pre-existing permeable joints.

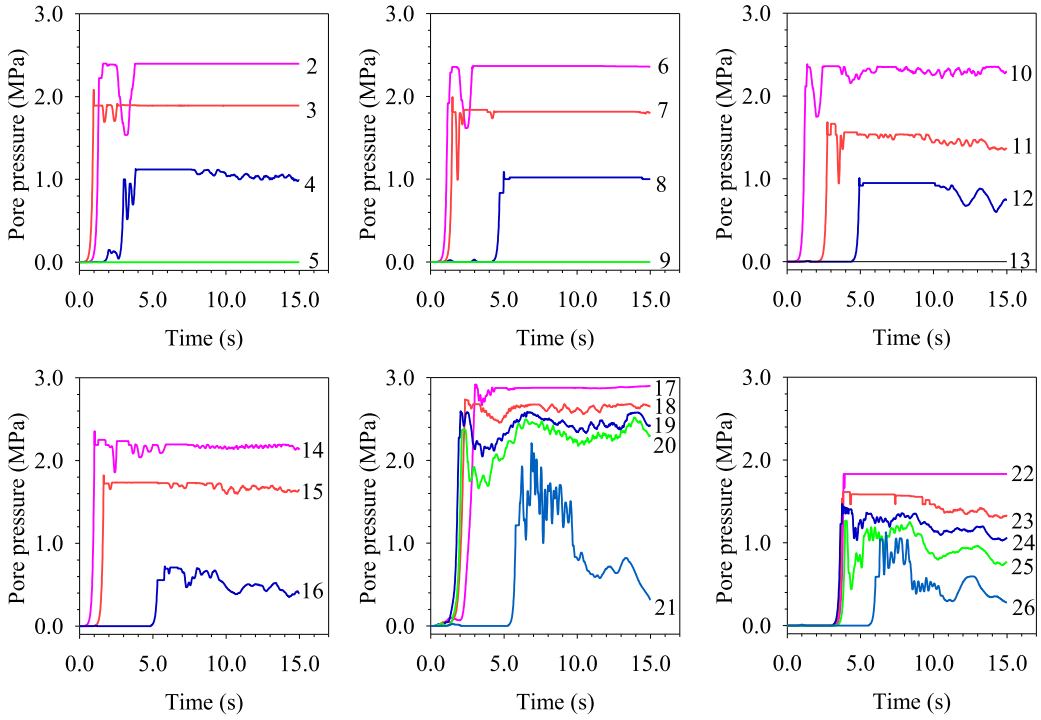

Fig. 29. Domain pore pressure vs. fluid flow time at different locations of Askara project.

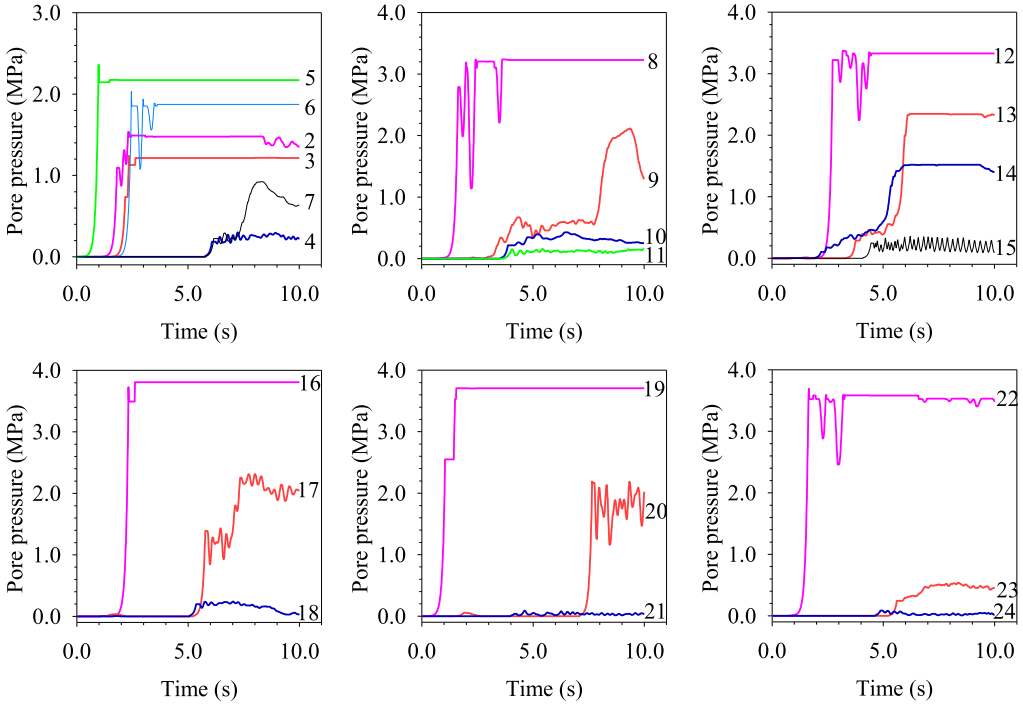

Fig. 30. Domain pore pressure vs. fluid flow time at different locations of Fossmark project.

8. Discussions

This section compares and highlights the reasons for the failure cases and the cases with success in the use of unlined pressure shafts and tunnels. The comparison is mainly made with the main focus on the engineering geological conditions of the cases, in situ stress state, fluid flow and groundwater conditions. These reasons will be the basis to enrich and develop the concept of favorable and unfavorable ground conditions for the applicability of the Norwegian confinement criteria in order to locate unlined pressure shafts and tunnels under constant hydrostatic head.

8.1. The cases of failure

It is highlighted here that at Herlandsfoss project, hornblende schist has very tight foliation joints almost parallel to the valley slope and consists of very few cross joints. The condition was favorable for unlined shaft and tunnel and there was no leakage occurring even though the maximum static water head is far above the potential groundwater table (GWT), as shown in Fig. 31a. On the other hand, excessive water leakage occurred in the outer part of horizontal high-pressure tunnel passing through weak mica schist. This is mainly due to the fact that the highly schistose foliation joints and prevailing cross joints were easy for the water at high pressure to make them open by hydraulic jacking. The joints along this stretch of pressure tunnel were filled with silt and clay and were easy for hydraulic jacking to occur. Further, the stress situation in hornblende schist at the tunnel level is relatively favorable because the location is at the level of valley bottom and the rock mass is strong enough to store the stress without failure. Opposite is the case with weak mica schist, since it is exposed more towards the valley side and hence stress anisotropy is more pronounced and de-stressing in Fig. 31a is very logical. Hence, the main causes for the failure in this case were relatively low rock cover (overburden) and weak and highly schistose rock mass.

In Byrte project, GWT is influenced by steep topography and major zone of weakness that almost follows the topographic slope (Fig. 31b). It is obvious that the hydraulic jacking and leakage occur at this inclined unlined pressure shaft since the de-stressing in the rock mass lying above pre-existing zone of weakness and GWT shall follow the zone, which is almost parallel to the topography and is at the near proximity of the surface. The major causes of the failure at this project were steep topography, presence of weakness and fault zones, and unfavorable jointing conditions.

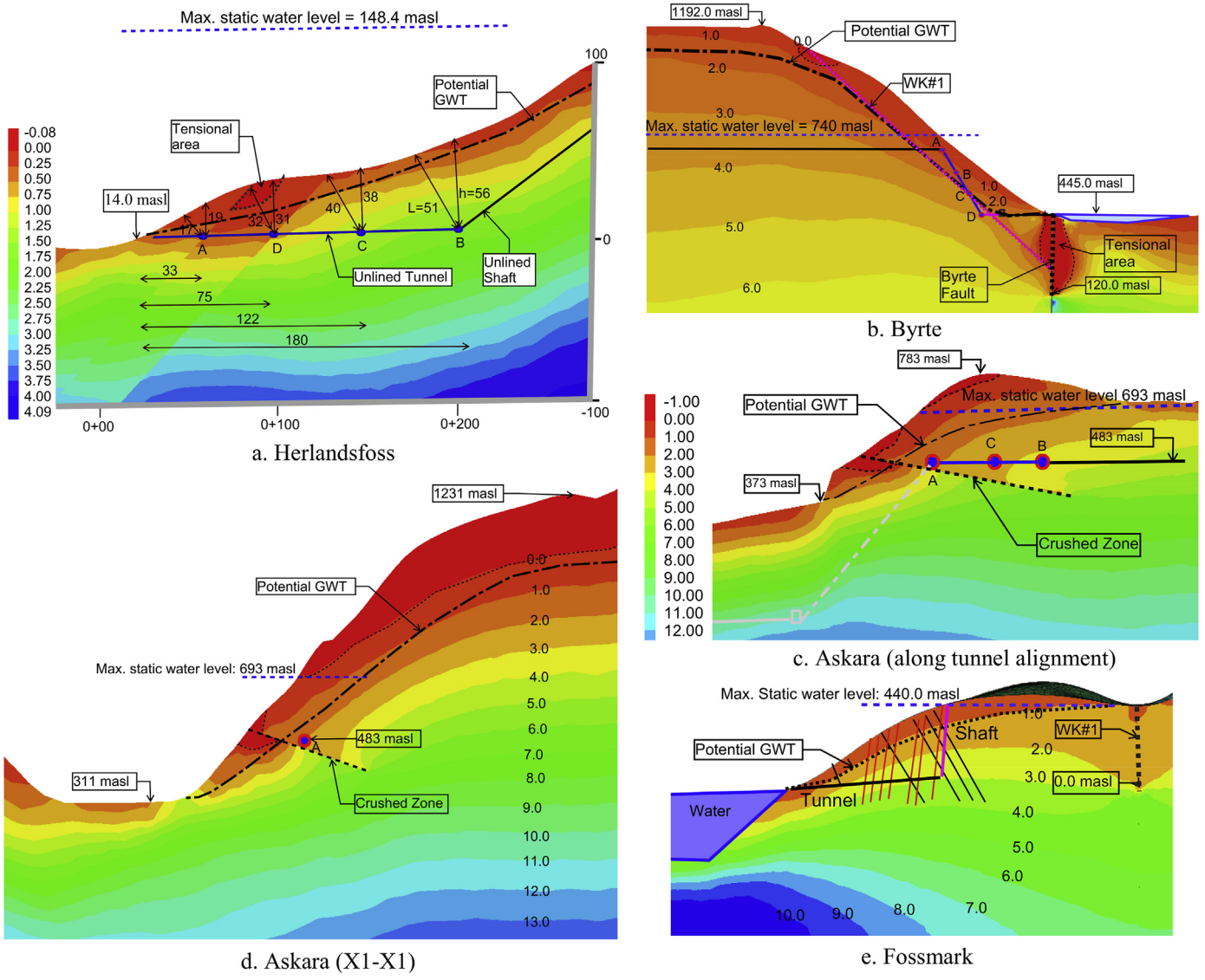

Fig. 31. Unlined shafts and tunnels with respect to groundwater table (GWT), minor principal stress (MPa), maximum static water level, zones of weakness, and joints.

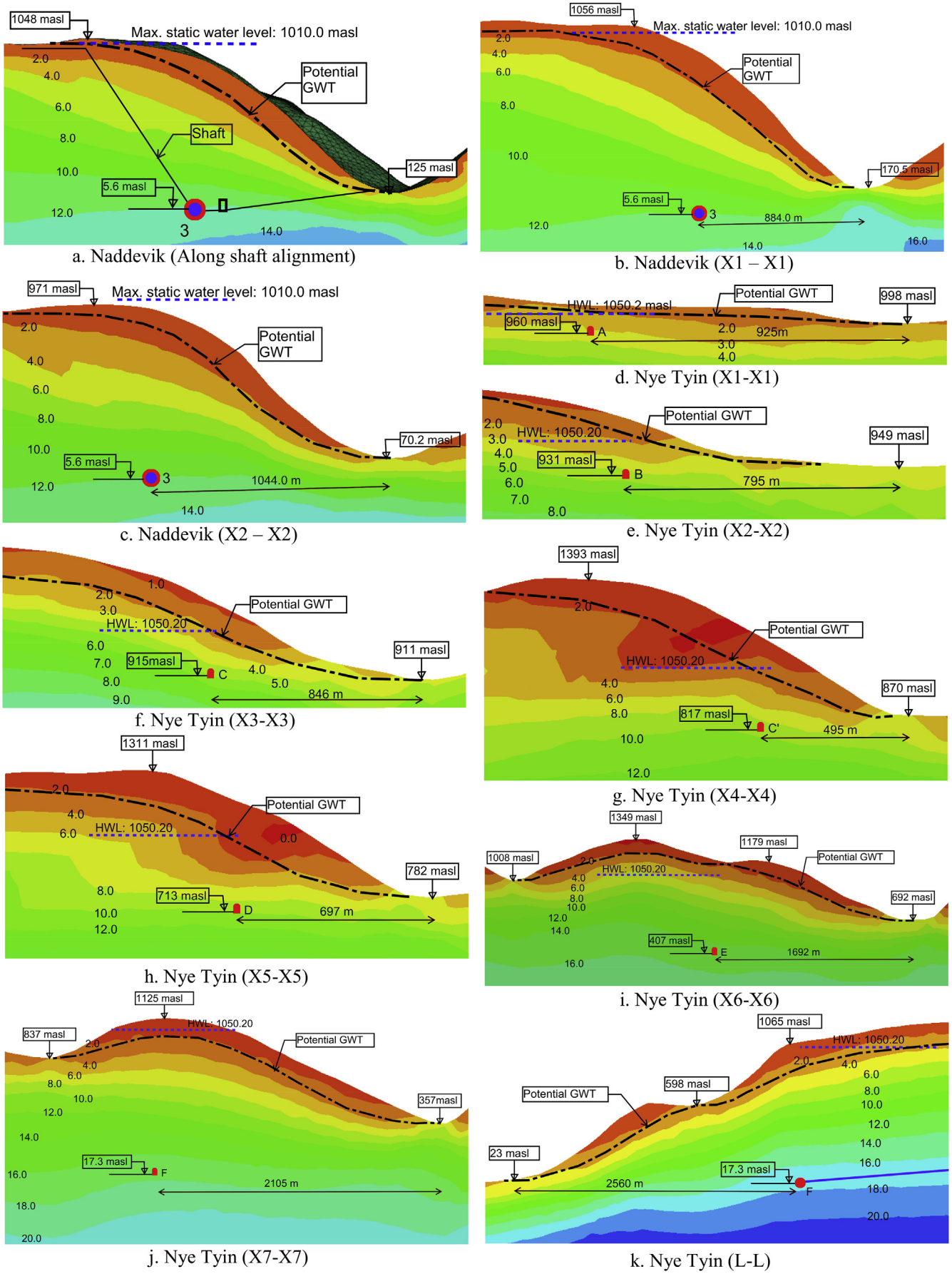

Fig. 32. Locations of unlined high-pressure shaft and tunnel along different sections of Naddevik and Nye Tyin projects (minor principal stress in MPa).

Table 8
Both favorable and unfavorable ground conditions for the applicability of Norwegian confinement criteria.

Category	Favorable conditions	Unfavorable conditions
Topography	Relatively gentle valley slope topography	Deep, steep and complex valley slope topography
Rock mass and jointing	Homogeneous and strong rock mass formations with no or single joint set having tight joint wall, wide spacing and anti-dip against valley slope	Weak rock mass with high degree of schistosity; Highly porous rock mass of volcanic and sedimentary origin; Jointed rock mass having more than two systematic and long persisting joint sets with one or more joint sets dipping steeply towards valley slope; Pre-existing open joints or the joints filled with sand and silt, which could easily be washed away; and sub-horizontal joints at low overburden area
Faults and weak/crushed zones	No nearby major faults and zones of weakness	Nearby fault and zones of weakness that are parallel or cross-cutting to the valley slope
In situ stress state	The minimum principal stress always higher than the static water head	De-stressed area and location not far away from steep valley slope topography; Not sufficiently far away from the locally overstressed areas
Hydrogeology	Hydrostatic water line below natural groundwater table or tunnel aligned deep into the rock mass and far away from the steep valley slope restricting flow paths to reach valley slope topography	Hydro-static line above the groundwater table and relatively near from the valley side slope; and Highly permeable and communicating joint sets

At the Askara project, the joints are steeply dipping and cross-cut each other at the fractured sandstone above the crushed zone (Fig. 31c and d). The crushed zone has considerable impact on the rock mass overlying above, which results in de-stressing in the fractured sandstone formation. The main failure phenomenon at this project is hence leakage through pre-existing joints, which have very low normal stress acting perpendicular to the dip. In addition, the failure location *A* is very near to the potential GWT. In summary, the failure in this case was mainly due to the presence of unfavorable topography, fractured rock mass with unfavorable jointing conditions, and crushed zone cross-cutting the shaft alignment.

At the Fossmark project, zone of weakness and steep topography with deep fjord valley influenced the stress state at the unlined pressure shaft and tunnel. Due to de-stressing, which leads to hydraulic jacking through pre-existing two cross-cutting joint systems, as shown in Fig. 31e, aggravated water leakage from the shaft and tunnel might occur. Hence, in this project, steep topography, deep fjord valley, zone of weakness parallel to the fjord valley and unfavorable jointing conditions were the main causes of the failure.

8.2. The cases of success

Different sections of both Naddevik and Nye Tyin projects are presented in Fig. 32 in order to build the concept of the successful placement of unlined high-pressure shafts and tunnels.

At the Naddevik project (Fig. 32a–c), the shaft bottom is located well below the valley bottom and the whole shaft alignment is considerably far away from the valley slope topography, leading to the increment in the stress confinement. In addition, there are no nearby pronounced faults and zones of weakness presented along the alignment and nearby area. Similarly, the rock formations mainly consist of Scandinavian hard rock composed of massive dark gneiss and granitic gneiss. There is almost no influence induced by the GWT, which should presumably follow the surface topography.

The pressure tunnel system of Nye Tyin project, on the other hand, passes through different rock formations consisting of relatively weak and micro-folded phyllite, mica schist and strong dark gneiss. The alignment of the pressure tunnel system at this project is located in such a way that the minor principal stress is considerably higher than the static head acting over it (Fig. 32d–k). However, favorability condition varies from location to location along this pressure tunnel system. One should note here that the pressure tunnel follows the alignment in such a way that the tunnel is always below the lowest point of the valley bottom and is considerably far away from it. Even at the tunnel segment where relatively weak phyllite and mica schist exist (Fig. 32d–f), the overburden cover exceeds 89 m and side cover is quite significant (85 m) in the relatively flat valley, which produces favorable in situ stress state. Similarly, the GWT is always above the hydro-static line, which hinders water to leak. On the other hand, one should note that the locations *C′* and *D* are somewhat critical since the tunnel is relatively closer to the valley side and valley slope is relatively steeper compared to the other part of the tunnel alignment (Fig. 32g and h). Still, as indicated in Fig. 32, the stress condition is quite favorable and the GWT is well above the maximum static water level.

8.3. Summary of discussions

It is important to summarize the common points and differences of the successful and failure cases. In doing so, both successful and failure cases are compared in terms of detail engineering geological assessment, stress state analysis, fluid flow analysis, potential groundwater conditions and Norwegian confinement criteria. The detailed analysis allowed us to suggest both favorable and unfavorable ground conditions for the applicability of the Norwegian confinement criteria and unlined high-pressure shafts/tunnel concepts beyond the Scandinavia. The different factors are summarized under each category of ground condition consisting of topography, rock mass, jointing and presence of faults and weak/crushed zones, in situ stress state and hydrogeology (Table 8).

9. Conclusions

Among more than 4000 km-long unlined tunnels and shafts so far built in Norway, the successful history is over 99% excluding few failure cases. The selected four failure cases were studied in detail considering engineering geological conditions, in situ stress state, hydraulic jacking and leakage potential. In addition, two successful cases of significance regarding the use of unlined high-pressure tunnel and shaft were also reviewed and analyzed. It is noteworthy to mention that along the analyzing process of this research, the news of operational failure came out from a newly constructed unlined high-pressure tunnel in Norway, indicating that the design of unlined pressure shafts and tunnels is very challenging. Aligning and placing the unlined pressure shafts and tunnels at a favorable conditions meeting all geological, geotectonic and hydrogeological aspects are complicated. Therefore, the

Norwegian design criteria for confinement cannot be directly copied to other geological and geotectonic environments. However, the authors are confident that the detailed review, analysis and assessment presented in this paper will certainly help users of unlined high-pressure shafts and tunnels concept to locate the alignment correctly with favorable ground conditions. It is highlighted that the confinement criteria must be supplemented with the detailed engineering geological assessment, stress state analysis, fluid flow analysis and hydrogeological analysis to make this concept a success outside the Scandinavia. It is emphasized here that no matter what the design methodology is used, the ultimate challenge in the design of unlined pressure tunnel/shaft is to ascertain the risk of hydraulic jacking/splitting, potential leakage and both short- and long-term stability of the tunnel itself.

Conflicts of interest

The authors wish to confirm that there are no known conflicts of interest associated with this publication and there has been no significant financial support for this work that could have influenced its outcome.

References

Barton N, Vik G, Johansen PM, Makurat A. Rock mechanics investigations for unlined pressure tunnels and air cushion surge chambers. In: Proceedings of the international conference on hydropower; 1987. p. 1–16.

Barton N. A review of the shear strength of filled discontinuities in rock. Oslo, Norway: Norwegian Geotechnical Institute (NGI); 1973.

Benson R. Design of unlined and lined pressure tunnels. Tunnelling and Underground Space Technology 1989;4(2):155–70.

Bergh-Christensen J, Dannevig NT. Engineering geological evaluations of the unlined pressure shaft at the Mauranger hydropower plant. Technical report. Oslo, Norway: Geoteam A/S; 1971.

Bergh-Christensen J, Kjolberg RS. Investigations for a 1000 m head unlined pressure shaft at the Nyset/Steggje project, Norway. In: Proceedings of the ISRM international symposium. ISRM; 1982. p. 537–43.

Bergh-Christensen J. Design of unlined pressure shaft at Mauranger Power Plant, Norway. In: Proceedings of the International Society for Rock Mechanics (ISRM) international symposium. ISRM; 1982. p. 531–6.

Bergh-Christensen J. Failure of unlined pressure tunnel at Åskåra Power Plant. In: Proceedings of the rock mechanics day; 1975. p. 15.1–8 (in Norwegian).

Bergh-Christensen J. Rock stress measurements for the design of a 965 metre head unlined pressure shaft. In: Proceedings of the ISRM international symposium. ISRM; 1986. p. 583–90.

Brekke TL, Ripley BD. Design guidelines for pressure tunnels and shafts. Technical report No. EPRI-AP-5273. Department of Civil Engineering, California University at Berkeley; 1987.

Broch E, Christensen J. Investigations of unlined pressure shafts. Trondheim, Norway: Norwegian Institute of Technology; 1961.

Broch E, Eslava LF, Marulanda A. Design of high pressure tunnels for the Guavio Hydroelectric Project, Colombia. In: Proceedings of the international conference on underground hydropower plants; 1987. p. 87–99.

Broch E. The development of unlined pressure shafts and tunnels in Norway. In: Proceedings of the ISRM international symposium. ISRM; 1982. p. 545–54.

Broch E. Underground hydropower projects - lessons learned in home country and from projects abroad. Norwegian Tunneling Society; 2013. p. 11–9.

Broch E. Unlined high pressure tunnels in areas of complex topography. International Water Power and Dam Construction 1984;36(11):21–3.

Buen B, Palmstrom A. Design and supervision of unlined hydro power shafts and tunnels with head up to 590 meters. In: Proceedings of the international ISRM international symposium. ISRM; 1982. p. 567–74.

Buen B. Documentation of unlined water conduits in Norway. Oslo, Norway: FHS; 1984. p. 75–85.

Edvardsson S, Broch E. Underground powerhouses and high pressure tunnels. Hyderopower development, vol. 14. Trondheim, Norway: Division of Hydraulic Engineering, Norwegian Institute of Technology; 2002.

Esteves C, Plasencia N, Pinto P, Marques T. First filling of hydraulic tunnels of Venda Nova III hydropower scheme. In: Proceedings of the world tunnel congress; 2017.

Fejerskov M, Lindholm C, Myrvang A, Bungum H. Crustal stress in and around Norway: a compilation of in situ stress observations. London, UK: Geological Society; 2000. p. 441–50.

Fejerskov M, Lindholm C. Crustal stress in and around Norway: an evaluation of stress-generating mechanisms. London, UK: Geological Society; 2000. p. 451–67.

Fejerskov M. Determination of in-situ stresses related to petroleum activities on the Norwegian continental shelf [Ph.D. Thesis]. Department of Geology and Mineral Resources Engineering, Norwegian University of Science and Technology; 1996.

Garshol K. Fossmark hydropower scheme, leakages from the unlined pressure shaft. In: Proceedings of rock blasting technology, rock mechanics and geotechnics; 1988. p. 25.1–25.11.

Geological Survey of Norway (NGU). National bedrock database. 2017. http://geo.ngu.no/kart/berggrunn_mobil/?lang =eng.

Hanssen TH. Investigations of some rock stress measuring techniques and the stress field in Norway [Ph.D. Thesis]. Department of Geology and Mineral Resources Engineering, Norwegian University of Science and Technology; 1997.

Hartmaier HH, Doe TW, Dixon G. Evaluation of hydrojacking tests for an unlined pressure tunnel. Tunnelling and Underground Space Technology 1998;13(4):393–401.

Hoek E, Carranza-Torres C, Corkum B. Hoek-Brown failure criterion - 2002 edition. In: Proceedings of NARMS-Tac; 2002. p. 267–73.

Hoek E. Rock mass properties for underground mines. In: Underground mining methods: engineering fundamentals and international case studies. Society for Mining, Metallurgy, and Exploration; 2001. p. 467–74.

Hydro. The new Tyin power system. Engineering geological report. Norsk Hydro ASA; 1998. Project No. ED1546.

Itasca. FLAC^{3D} 5.0 user's manual: interfaces. Itasca; 2017a.

Itasca. UDEC 5.0 user's manual: fluid flow in joints. Itasca; 2017b.

Johansen T. Norwegian tunneling. Oslo, Norway: FHS; 1984.

Kestin J, Sokolov M, Wakeham WA. Viscosity of liquid water in the range − 8 °C to 150 °C. Journal of Physical and Chemical Reference Data 1978;7(3):941–8.

Lamas LN, Leitao NS, Esteves C, Plasencia N. First infilling of the Venda Nova II unlined high-pressure tunnel: observed behaviour and numerical modelling. Rock Mechanics and Rock Engineering 2014;47(3):885–904.

Liu K. Stress calculation of unlined pressure tunnel surrounding rock in hydraulic engineering. In: Instrumentation and measurement, sensor network and automation (IMSNA). Institute of Electrical and Electronics Engineers; 2013. p. 57–60.

Marwa EM. Geotechnical considerations in an unlined high pressure tunnel at Lower Kihansi in Tanzania. Bulletin of Engineering Geology and the Environment 2004;63(1):51–5.

Ming L, Brown ET. Designing unlined pressure tunnels in jointed rock. International Water Power and Dam Construction 1988;40(11):37–41.

Myrset O, Lien R. High pressure tunnel systems at Sima power plant. In: Proceedings of the ISRM international symposium. ISRM; 1982.

Myrvang A. Personal communication with Arne Myrvang on 15th February 2017. 2017.

NGI. Overview of Norwegian unlined tunnels and shafts with water pressure over 100 m and some others with lower pressures. Oslo, Norway: NGI; 1972.

Nilsen B, Thidemann A. Rock engineering. Trondheim, Norway: Division of Hydraulic Engineering, Norwegian Institute of Technology; 1993.

Norconsult. Alto Maipo hydropower. 2017. https://www.norconsult.com/references/energy/alto-maipo-hydropower.

Norges Vassdrags og Elektrisitetsvesen (NVE). Byrte power plant: failure in pressure shaft. NVE; 1970.

Palmstrom A, Broch E. The design of unlined hydropower tunnels and shafts: 100 years of Norwegian experience. International Journal on Hydropower and Dams 2017;(3):1–9.

Palmstrom A. Norwegian design and construction of unlined pressure shafts and tunnels. In: Proceedings of the international conference on hydropower in Oslo, Norway; 1987. p. 87–111.

Panthi KK, Basnet CB. Design review of the headrace system for the Upper Tamakoshi project, Nepal. International Journal on Hydropower and Dams 2017;1:60–7.

Panthi KK, Basnet CB. Review on the major failure cases of unlined pressure shafts/tunnels of Norwegian hydropower projects. Journal of Water, Energy and Environment 2016;18:6–15.

Panthi KK. Norwegian design principle for high pressure tunnels and shafts: its applicability in the Himalaya. Journal of Water, Energy and Environment 2014;14:36–40.

Rocscience. Estimating joint stiffness. 2017. https://www.rocscience.com/help/phase2/webhelp9/theory/Estimating_Joint_Stiffness.htm.

Selmer-Olsen R. Experience gained from unlined high pressure tunnels and shafts in hydroelectric power stations in Norway. Norwegian Soil and Rock Engineering Association; 1985.

Selmer-Olsen R. Experience with unlined pressure shafts in Norway. In: Proceedings of the international symposium on large permanent underground opening; 1969.

Selmer-Olsen R. Underground openings filled with high-pressure water or air. Bulletin of the International Association of Engineering Geology 1974;9(1):91–5.

SINTEF. Rock mechanical properties. SINTEF Building and Infrastructure; 1998. Report No. STF22 A98034.

SINTEF. Rock stress measurements at the Nye Tyin hydropower project. SINTEF Building and Infrastructure; 2002.

Valstad T. Unlined water tunnels and shafts: water leakage from headrace tunnel of Bjerka power plant. Oslo, Norway: NGI; 1981 (in Norwegian).

Vik G, Tunbridge L. Hydraulic fracturing - a simple tool for controlling the safety of unlined high pressure shafts and headrace tunnels. In: Proceedings of the ISRM international symposium. ISRM; 1986.

Vogt JHL. Pressure tunnels and geology. Technical Report No. 93. Oslo, Norway: NGU; 1922.

Chhatra Bahadur Basnet is conducting his PhD research at the Department of Geoscience and Petroleum, Norwegian University of Science and Technology (NTNU), Norway. His current research work is related to unlined pressure tunnels in hydropower projects. He holds MSc degree in Hydropower Development from NTNU. He has more than six years of working experience in planning, design, and construction supervision of numbers of hydropower projects in Nepal.

Krishna Kanta Panthi is an Associate Professor in Geological Engineering at the Department of Geoscience and Petroleum, Norwegian University of Science and Technology (NTNU) since 2008. He holds the degrees of PhD in Rock Engineering, MSc in Hydropower Engineering and MSc in Tunneling. He has approximately 25 years of experience in design, construction management and research of tunneling, hydropower, slope stability and mining projects. He is the author of many scientific papers published in renowned international journals.